The Application of Recycled Polypropylene in Active Closures

Tiancheng Guo

Faculty of Mechanical, Maritime and Materials Engineering (3mE)

TU Delft Delft University of Technology

Challenge the future

The Application of Recycled Polypropylene in Active Closures

by

Tiancheng Guo

in partial fulfillment of the requirements for the degree of

Master of Science
in Materials Science and Engineering

at the Delft University of Technology,
to be defended publicly on Jan. 25th, 2022.

Student number:	5006783	
Project duration:	Apr 3rd, 2021 – Jan 19th, 2022	
Thesis committee:	Dr. M. A. Bessa,	TU Delft
	Dr. A. M. Aragón,	TU Delft
	Dr. Henk den Besten,	TU Delft
	Ir. Bas den Boer,	Weener Plastics
	Ing Ruben Clerx,	Weener Plastics

An electronic version of this thesis is available at http://repository.tudelft.nl/.

TU Delft Delft University of Technology

ABSTRACT

Polymers have a long history of development and their application widely supports the normal operation of industry and society. Yet, the environmental consequences of using virgin plastics demand new sustainable solutions. In this quest, being capable of predicting the mechanical behavior of post-consumer recycled plastics is essential to support the adoption of these materials in engineering applications. This literature review focuses on recycled polypropylene and its mechanical viability when used in closures, a common part in packaging industry. Recycled polypropylene's performance is found to be dependent on crystallinity, which in turn is dependent on the length of the polymer chains, isotacticity and other co-polymerization segments. This document also reviews constitutive models applicable to predict the behavior of closures via the the finite element method. A suitable thermo-viscoplastic model is selected, setting the stage for the finite element analyses to be conducted during the dissertation work.

The application of recycled polypropylene is challenging due to its low mechanical properties. In the thesis, we demonstrate the possible aspects which decide the properties of post consumer recycled polypropylene (PCR-PP), including molecular weight, tacticity, interface structure and degradation. After discussing the material properties, the focus is to testify the application of PCR-PP in closures for particular functionality. For active closures, the weakest structure is the hinge, at the middle of lid. To verify if the material is applicable to active closures. Finite element analysis are conducted to help develop new products in a more efficient way, and also reduce the plastic waste.

In the thesis, the explicit dynamic method and the static general method are applied with different boundary conditions in the model to simulate the differentiation of closures including manufacturing conditions. The explicit dynamic simulation involves higher computational cost, and due to the existence of inertial effect, the observed reaction force is significantly higher than it should be when the mass scaling is over a certain region. Considering an implicit static analysis was found to be proper. Once the loading condition was simplified and by carefully choosing an propriate thermo-visco-plastic constitutive model, the finite element analysis can predict the snap through behavior of the closure. The snap-through behavior also shows that the equivalent plastic strain at the hinge middle is higher than the maximum tensile strain of polypropylene(QCP-300P) under room temperature. However, when subjected to 69 degree Celsius, the closure is expected to deform without failing. This result demonstrate the necessity of bending the closures right after injection molding, which fit with the experimental result.

CONTENTS

1

INTRODUCTION

In 1867, the first human-synthesised plastic was introduced to the public by John Wesley Hyatt. John invented a type of plastic by treating cellulose with camphor[1]. Later in 1907, Leo Baekeland invented Bakelite which is regarded as the first fully synthetic plastic without molecules found in nature. Beside being applied as an effective insulator, Bakelite exhibits other properties, including durable, heat resistant, and ideally proper for mass production. The production of plastics grows rapidly, especially after mid twentieth century.

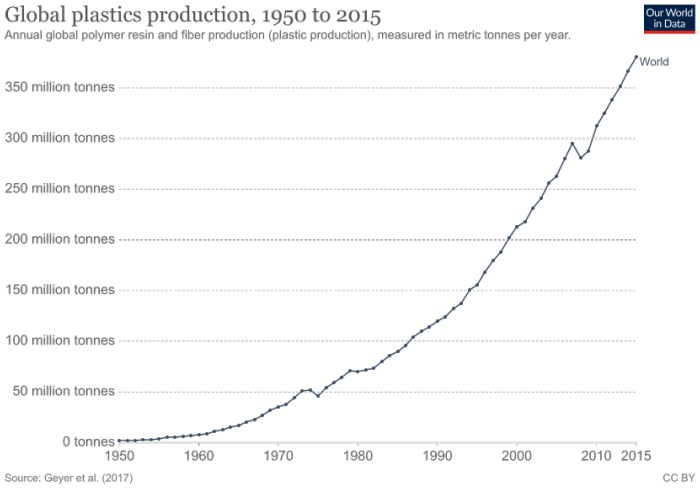

Figure 1.1: World Plastic Production Statistics[1].

Later in the 1970s, Plastic's reputation dept because of the waste increase[1]. So many disposable plastic products are buried in the environment. At the moment, there is no alternative that is cheap, available and flexible for industry. After debates and arguments, the plastics industry began to seek for recycle solution for the products. 10 years later, the plastics industry played a role in encouraging municipalities to collect and process recyclable materials as part of their waste management system. In fact, recycling is still far from perfect, and most plastics still end up in landfills or the environment. The details of recycling would be discussed in later chapters.

An important member of the plastic's group, polypropylene is widely used in various products around the world. It gains its popularity from its competitive properties.

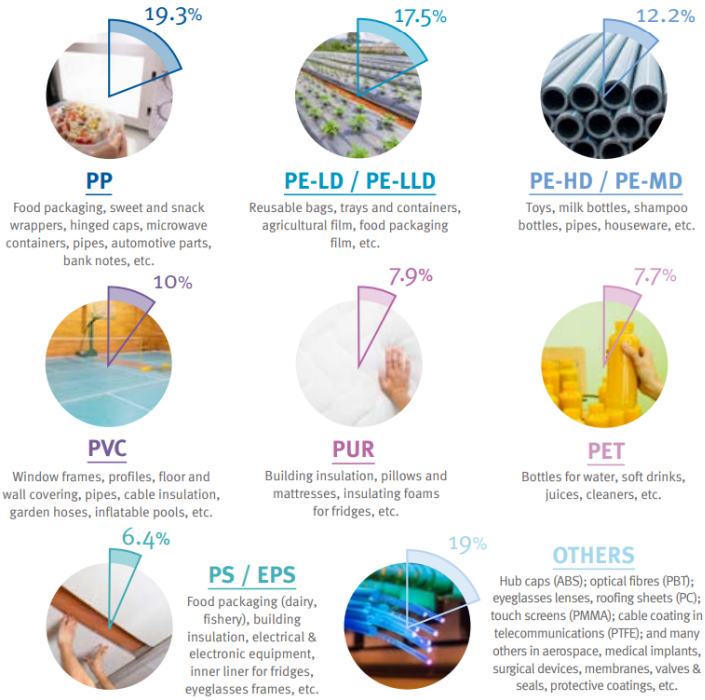

Figure 1.2: The static data of plastics demand distribution by resin types in Europe[2].

After the synthesis of its resin in 1954, the polypropylene rapidly drew attention from the industry because of its low density[1]. Polypropylene is widely used in packaging and many other fields, such as automotive industry, special devices. In 2018, PP accounted for 19.9% of total plastic consumption in Europe[2]. To avoid further destruction to environment from plastic products, the recycling technology for plastic gains its necessity.

This thesis focuses on investigating the use of recycled PP at hinges, a very thin sheet-like structure, which need to be bent without breaking, even it works through 180° rotation. In addition, the hinge is active, i.e. they need to close by themselves without being compressed by the thumb. The property indicates that the target products may including a certain instability in its design because of buckling effects. Compared with the simplest polyethylene, polypropylene has one more methyl group on the side chain of each monomer.

1.1. EFFECTS OF RECYCLING POLYPROPYLENE

1.1.1. OVERVIEW ON POLYPROPYLENE

As a polymer with side chains, different to polyethylene, the molecular structures of PP are divided into different groups when the monomers are limited to be propylenes. Upon polymerization, it's possible for PP to form three basic chain structures depending on the position of the methyl groups. When methyl group stays in irregular sort, the polymer is

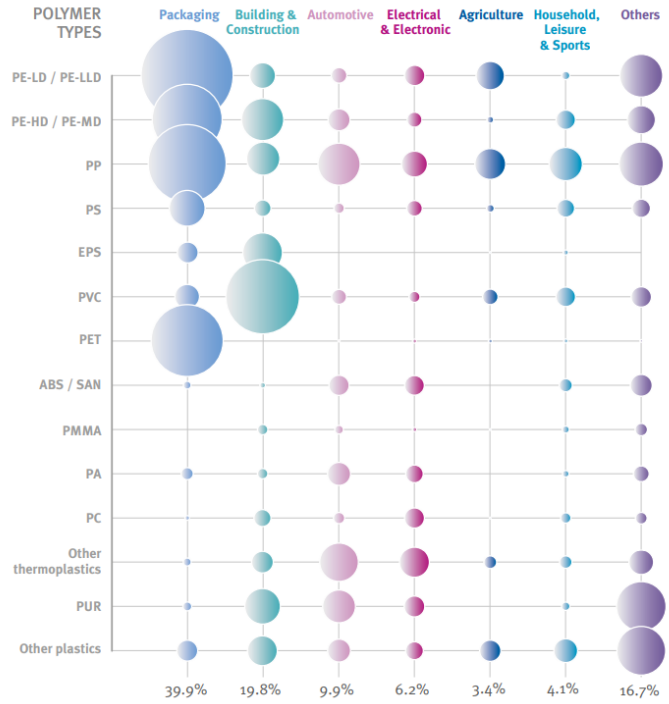

Figure 1.3: The plastic demand by segments and polymer types in 2018[2].

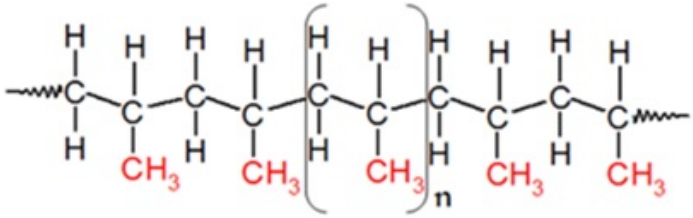

Figure 1.4: molecular structure of polypropylene[3]

defined as atactic polypropylene (aPP). Isotactic PP implies that all methyl groups are at the same side of carbon chain, which means all monomers are polymerized at same status. In addition to these two types, if any adjacent polymer chain unit has opposite side chain positions with its neighbors, then the polymer will be called syndiotactic PP (sPP).

All three types of polypropylene belongs to the polypropylene homo-polymers, which occupy 65-75% of the market [4]. Polypropylene co-polymer has two main types in the market. Block co-polymer polypropylene owns co-monomer units, such as ethylene, which are arranged in blocks. The ratio of co-monomer units are typically around 10%. The other type of monomers improves certain properties, like impact resistance while other additives enhance other properties. Random co-polymer polypropylene, different to block co-polymer polypropylene, has the co-monomer units arranged in random segments along the polypropylene molecule. Random co-polymer polypropylene are usually combined with 1% to 7% ethylene. Based on it's properties, random copolymer polypropylene is selected for more malleable applications. In addition, the mixture of Homopolymers polypropylene and 45%-65% polyethylene is defined as impact modified copolymer.

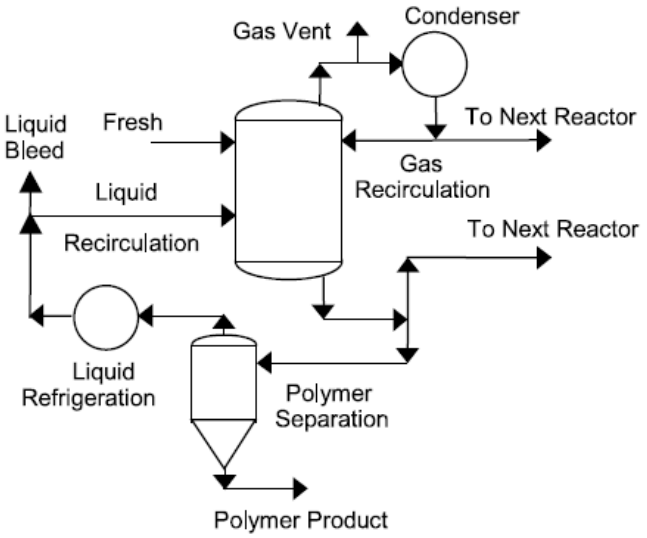

Figure 1.5: slurry method of polypropylene production[4].

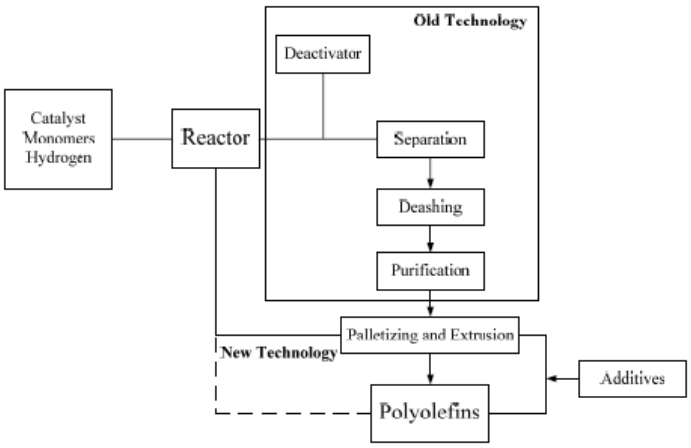

Figure 1.6: traditional process of polyolefin production.png[5].

1.1.2. SYNTHESIS OF POLYPROPYLENE

Before discuss the structure-properties relationship of PP materials, it's necessary to have a summary of the producing of PP.

The first commercial production of polypropylene was after the discovery of the Ziegler-Natta catalyst in the 1950s. It was originally produced by the slurry method. Propylene, solvent and catalyst are placed in series reactors. The polymerization reaction is carried out under reaction conditions of 160°C to 175°C and 0.39 to 0.71 MPa. The polymer solution is diverted into the evaporator to remove solvent and propylene, generating a mixture of crystalline and amorphous polymer. The disadvantage of this route is that the catalyst must be treated with alcohol to deactivate and extract it, while the unwanted atactic polymer must be extracted and removed. Due to the high proportion of atactic polypropylene in this production process, the production cost is high.

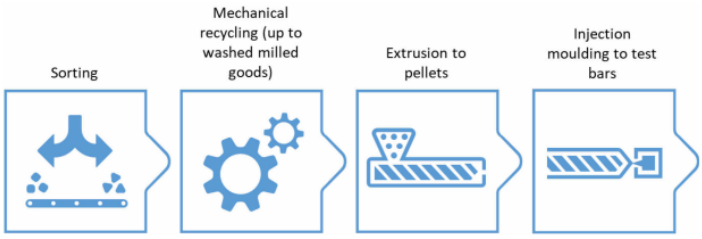

Figure 1.7: mechanical recycling procedure of PP[6].

After further development, the applicable polymerization processes are introduced to the industry. In addition to the solution method described above, the production methods of polypropylene include gas phase method and bulk method. Among these three mainstream methods, the liquid bulk method has shown the advantage of high conversion rate. The bulk method uses liquid propylene as the reaction medium and raw material, avoiding the interference of extra solvents in the slurry method. Under the action of the catalyst, the reaction is performed at a lower temperature and a higher pressure. After the propylene and catalyst are recovered, granulated polypropylene products are obtained through granulation. In this production process, the proportion of atactic polypropylene is greatly reduced, which accounts for only 5% of the total product. In the hexane solvent, because the solubility of isotactic polypropylene and atactic polypropylene are different, they can be separated by extraction. The isotacticity of polypropylene is defined as the mass fraction of undissolved solids in the total product.

1.2. RECYCLING OF PP MATERIALS

As a major type of thermoplastic, polyolefin is used worldwide. Many common plastic products are produced from polyolefin materials. In Western Europe alone, these three polymers consume about 21.37 million tons per year, accounting for 56 percents of thermoplastic material [2].

1.2.1. RECYCLING METHODS

Unlike condensation polymers, thermoplastics cannot be recycled easily through simple chemical methods . This feature stems from the irreversibility of addition polymerization. Generally speaking, for the recycling of polypropylene materials, there are several different ways to choose from. On the one hand, by creating a high-temperature environment, long-chain polymers will undergo covalent bond breakage, resulting in thermal cracking products such as small molecular olefins. These decomposition products can be used in industry to re-synthesize other products. Different methods could be applied to realize the purpose, including thermal cracking method, mechanical method, and dissolution/re-precipitation method.

MECHANICAL RECYCLING METHOD

As the most applicable recycling method in worldwide, the later discussion of the PCR-PP properties would based on mechanical recycling technique. Mechanical recycling refers to operations that aim to recover plastics via mechanical processes (grinding, washing, separating, drying, re-granulating and compounding), thus producing products that can be converted into plastics products, substituting virgin plastics. It is also known as material

recycling, material recovery or, related to plastics, back-to-plastics recycling. In mechanical recycling, plastic waste (sorted by material type) is milled and washed, passes a flotation separation, and is dried. The plastic flakes are then either used directly to produce new plastic materials or they are processed into granulates beforehand. Mechanical recycling is used for the recovery of pre-consumer (post-industrial) material as well as for post-consumer plastic waste. It is currently the dominating method of recycling post-consumer plastic waste in Europe. For mechanical recycling, only thermoplastic materials are of interest, i.e. polymeric materials that can be re-melted and re-processed into products via techniques such as injection moulding or extrusion. It is a well-established technology for the material recovery of plastic materials such as polypropylene (PP), polyethylene (PE) or polyethylene terephthalate (PET).

The cost of perfectly filtering is rather high for mechanical recycling. Many products are manufactured in a way that makes it difficult to separate the plastic components, which makes them difficult to recycle. For example, for a commodity, it may be assembled from different types of plastic parts. Such as a water bottle with a cap or a ballpoint pen. For their users, it is not realistic to clearly distinguish different types of materials and to finely sort waste, because this requires professional knowledge. What is even more troublesome is that for some diaphragms or packaging materials, various polyolefins (polypropylene and polyethylene) are often used in multiple layers, resulting in various plastics being mixed. Traditionally, the cheapest way for companies to filter different types of plastic waste is the soaking method. The density of the plastic materials varies from type to type, as a result, a large difference of density between two types of materials push them to stay at top or bottom of the solvent. Obviously, under the condition when plastic has similar density, it would not be able to sort them out. Researchers has made efforts to improve the filtering efficiency of plastic recycling. Silvia Serranti et al. evaluate a recycling process to obtain high quality polypropylene and polyethylene as secondary raw materials [7]. The technique is based on magnetic density separation (MDS) and hyperspectral imaging (HSI). The origin of MDS technique is also based on the density difference among materials, but highly improve the accuracy. While, as it mentioned, the cost of new techniques involved in the procedures would significantly accumulate more financial cost for the whole recycle system. So there is a trade between the cost and the quality of r-Plastic. In the later chapter, the discussion based on how to predict the mechanical behavior of the r-PP, which might improve the application status of r-PP based on limited financial support.

THERMAL CRACKING RECYCLING METHOD

According to the definition, thermal cracking recycling method could be defined as a tertiary recycling method. By rising temperatures, it's possible to decompose PP materials into different thermal cracking products by adjust the temperature range[8]. At 700 °C , polypropylene is decomposed into aromatic compounds. And if the thermal cracking happens at 400-500 °C, the products are gas, condensate hydrocarbon oil and waxes.

DISSOLUTION/RE-PRECIPITATION METHOD

Dissolution/re-precipitation method belongs to secondary recovery methods. A solvent technique has been developed whereby polypropylene may be converted to a form suitable for reprocessing. The method involves dissolution of the polymer in a suitable solvent

with subsequent polymer recovery and drying to produce a free-flowing powder. The solvent recycling method allows conversion of the polymer to a suitable form for reprocessing without significant degradation of the polymer. That is, degradation was not evident in the dissolution and drying stages. Degradation on recycling is then controlled by the reprocessing technique adopted. Reprocessing by extrusion of the stabilised polymer caused only limited degradation. The solvent recycling technique, however, reduces the stabiliser content of the polymer which may have an effect on film lifetime.

1.2.2. CHALLENGES TO RECYCLE PP MATERIALS

This review will not consider bio-compatibility, safety and other factors. It focuses on changes in mechanical properties. According to the report of Official Energy Statistics from the US Government[9], the amount of Polypropylene produced is 2.58 million tons while the recycling amount is only 130 thousand tons. Such a low recovery rate is due to the high process cost compared to the cost of producing polypropylene (PP). Economic constraints limit the further separation or the application of expensive additives in recycle progress[9].

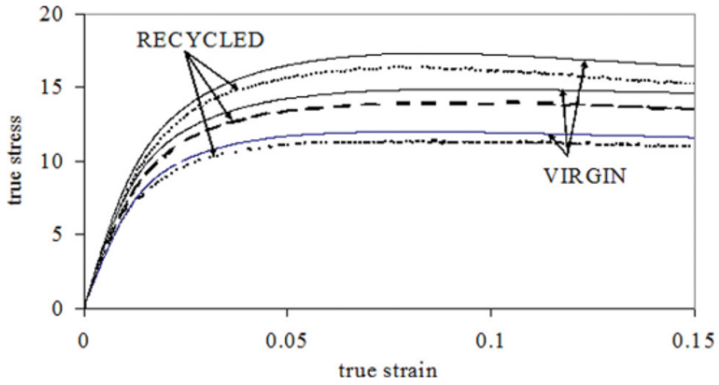

Figure 1.8: Recycling effect on the true stress-strain curve of PP under different strain rates[10].

The decrease of mechanical properties is a key reason to limit the application of post-consumer polypropylene (PCR-PP) in structures. According to the research of Daniel Pessey in the figure [10],the elastic properties are not significantly effected when comparing i-PP's property before and after the mechanical recycling procedure. However, they find that the drop of plasticity influence the behavior of the material.

Notwithstanding the poor performance compared to virgin polypropylene, the properties of recycled PP could also vary with different batches[11][12]. According to the research of M. Raj et al, recycled PP's tensile properties of different batches are not stable[13]. The data obtained from the tensile tests indicate that the third reprocessed material shows lower tensile properties compared to the first and second reprocessing. In addition, the durability and recycling potential are quite different among batches. It is unacceptable for manufactures to use materials with unstable properties. Jansson et al analyzed the performance of recycled PP materials through simulation experiments, and used simulated recycling test procedures to check and compare two PCR-PP. It consists of repeated cycles of alternating extrusion and accelerated thermal oxidation aging [14]. In each aging step, the

elongation fluctuation due to subsequent extrusion. In addition, the combination of extrusion and aging lead to a faster degradation of the material than aging or repeated extrusion alone. The researchers give the following three speculations to explain the difference in PP material properties. First, this may be due to the change of crystallinity, second, to surface degradation, and third, the dilution of degraded polymer chains after re-extrusion. They speculate that the performance difference may be due to a combination of the above three reasons.

Furthermore, the cost of separating mixed plastics is an important reason limiting the commercial success of any recycling technology. The problem is that the price of virgin plastic may be lower than the plastic recycled after consumption. Consumers that refuse to pay a premium for recycled parts, or refuse to accept parts whose performance or quality is inferior to that of virgin resin or recycled parts with poor performance[2].

1.3. STRUCTURE - PROPERTIES RELATIONSHIP OF PCR-PP

PCR-PP exhibits degradation of mechanical properties when compare to virgin PP. The behavior of the PCR-PP related to the uncertain origin of plastic waste and the way to recycle or to simulate the recycling procedure. Understanding what happens to PCR-PP requires focusing on what happens to homo-polypropylene at beginning. PCR-PP has simple polymer structure, without comprehensive side chains and various chemical bonds on the main chain. For pure h-PP materials, the basic properties explaining degradation in mechanical behaviors of r-PP include molecular weight and tactility.

The sequence and classification of sub-chapters are based on the following order: the properties of pure r-PP, the properties of r-PP blends, the other additives, manufacturing conditions.

1.3.1. CRYSTALLINITY AND PHASE STRUCTURE

The common factor that determines the mechanical properties of PCR-PP is crystallinity[15]. Solid matter has two basic condensed states, crystalline state and amorphous state. The amorphous state can also be called the glass state. When in the crystalline state, the molecules are organized and fixed in a three-dimensional ordered periodic sequence[15]. In this case, the system has the lowest thermodynamic energy and is in a stable state. This is not only a characteristic form of ceramics or metal materials, but also one of the existing forms of high molecular polymers. Some polymers can exist in a crystalline state, while some polymers can only exist in an amorphous state. There are two conditions for determining whether a polymer will crystallize. One is the appropriate temperature, which is no different from small molecule materials. On the other hand, the regularity of the molecular chain structure. Polymers with structural regularity can be crystallized under certain conditions, and such polymers are also called crystalline polymers. However, it should be noted that the crystallization of polymers is not an absolute concept, because for most crystallizable polymers, their crystallization process is a result of tropism. Polypropylene under normal circumstances will not be completely crystalline or amorphous[16]. Therefore, when discussing the crystallization of materials, researchers introduced the concept of crystallinity. The degree of crystallinity is described as the percentage of crystalline material to the mass

of the total material. Different polymer structures, different molecules, and different cooling methods will all lead to different crystallinity.

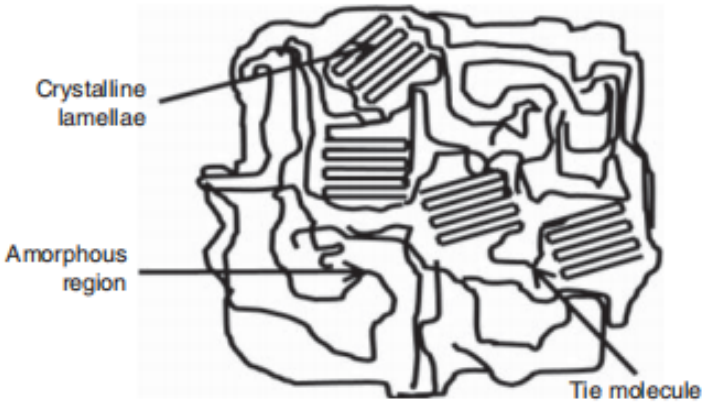

Figure 1.9: crystalline structure of polymer[17].

The figure shows the crystalline model of semi- crystalline polymer. The system will be completely crystalline only under conditions of infinite heat exchange that tends to zero, otherwise it will be in the situation shown in the figure. When the reversibility of the heat transfer process decreases, the relatively unstable amorphous state tends to expand. In the thermodynamically stable region, because the molecules are highly crystallized, the van der Waals force is at its maximum, so it exhibits higher stiffness when subjected to external stress, that is, it has a higher Young's modulus and a greater yield stress. At the same time, because the polymer chain segments are fixed at the position under the crystalline structure, based on the inter-molecular force provided by the periodic structure, the resistance that needs to be overcome when the adjacent polymer chains undergo relative displacement will increase. This phenomenon can be explained from the perspective of thermodynamics. A system with a high degree of regularity has a lower entropy than a system with a low degree of regularity. According to the Gibbs free energy equation, in a thermodynamic process, the thermodynamic energy barrier and entropy become negatively correlated. The conversion from a low-entropy state to a high-entropy state requires additional work from the external system. Therefore, compared with amorphous polypropylene, polypropylene materials with higher crystallinity are more difficult to undergo plastic deformation, and the maximum elongation strain is smaller on the stress-strain curve. Later we will analyze how the relative molecular weight and crystallinity parameters affect crystallinity.

MOLECULAR WEIGHT

Crystallinity is a secondary property for materials, which means it is controlled by other factors, including the manufacturing conditions, self-properties of the materials[18, 19]. The molecular weight of the polymer is one of the most basic factor which decide the material behavior. In recent years, researchers has carried out relative experiments to test the relationship between the molecular weight and properties of PP[17, 20–22]. However, most of the research concerned on the effect between molecular weight and rheological properties, such as viscosity. The discussion about how the molecular weight affect the tensile/-

compression behavior are relatively rare. Still, the published results prove the existence of relationship between molecular weight and stress-strain curve.

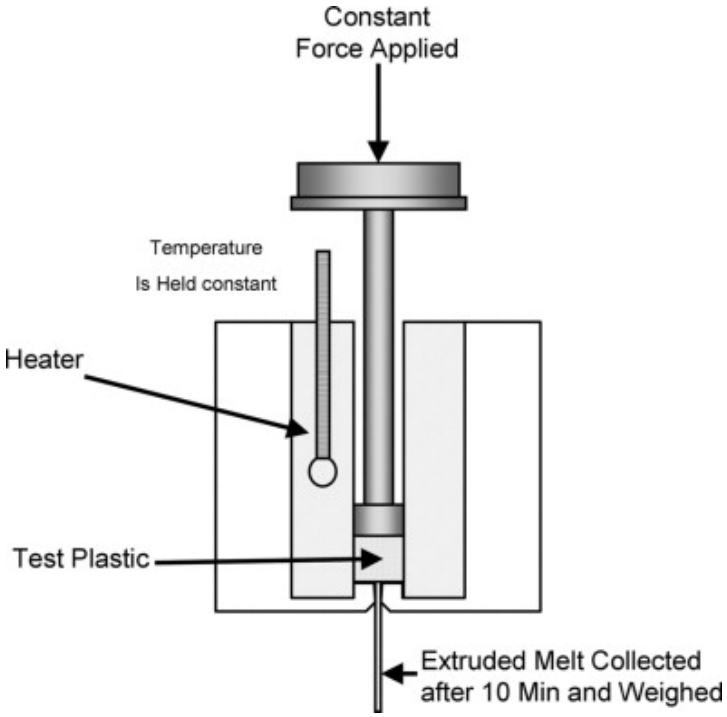

Figure 1.10: Test of Melt Flow Index.png[23].

In actual industrial applications, the cost of accurately measuring the relative molecular mass of polymers is too high, so MFI (Melt Flow Index) is specified as the grade of polymers The MFI is a numerical value representing the flow properties of plastic materials during processing. The MFI measurement method is generally measured according to the method specified in ASTM D1238. Its principle is to put plastic or resin into a metal sleeve with a fixed inner diameter, and heat the plastic or resin into melt, and then apply a load to the piston, comparing the extension of molten plastic through a small hole, and calculating the weight of the plastic extruded. This method can also be used to measure melt density, viscosity, shear stress and other properties.

MFI has a correlation with relative molecular mass[24]. As the type of materials are set as polypropylene, based on Pouiselle Equation[24].:

According to this model, when the environmental parameters are unchanged for a given material, the MFI obtained from the measurement results is not only a rheological parameter, but also can represent the relative molecular mass, the two are reciprocal . The larger the MFI, the smaller the relative molecular mass. In this way, the conclusions in the literature that discuss the relationship between material grade and mechanical properties can also be understood as how the relative molecular mass of the material affects the tensile mechanical curve. In addition, when we get a suitable range of relative molecular mass, we can also convert it to grade according to the calculation result, which can be used to guide the selection of materials in industrial production.

$$\text{Melt viscosity, } \eta = \frac{\pi P r^4}{8QL}$$

$$\text{Melt index} = \text{MI} = k\sigma Q$$

$$\text{MI} = \frac{K}{\eta}$$

where σ = polymer density, g/cm^3
Q = polymer volumetric flowrate, cm^3/s
k = 600 s/(10 min)
P = pressure, g/cm s^2(dynes)
R = die orifice radius, cm
L = orifice length, cm
η = melt viscosity, g/cm s (poise)
$K = \frac{\pi k \sigma P R^4}{8\eta L}$

Researchers from different groups reported similar tendency of how molecular weight influence the mechanical behavior of PP. The study of Toshio Ocawa [25], verifying the widespread empirical formula p = A + B/M for plastic products. Where P represents the mechanical properties, A and B are empirical parameters, and M is the average molecular mass. It should be noted here that A and B are numerical parameters, so the sign of B determines the sign of the correlation between molecular mass and mechanical properties. The interesting result is that the B parameter is positive in the flexural test and negative in the tensile test. This result indicates that the increase in relative molecular weight promotes the tensile properties of the material, but inhibits the improvement of compression performance.

Jmal et al. test the tensile behavior of different grades r-PP[26]. The three tests from left to right of the same sample represent faster and faster stretching rates. The indexes 3,10,54 here stands for the grade of material. The comparison shows that the PP-3 sample with the lowest grade has the greatest ductility and exhibits much greater strain than the other two r-PP samples at a lower stretching rate. At the same time, even if the stretching rate is increased, the PP-3 sample can still maintain a good elongation rate. This shows that for different materials of the same polypropylene, the material with a lower grade has better ductility. In addition, the researchers changed the grade by adding polyethylene to r-PP. This proved that in addition to directly changing the relative molecular mass, changing the system composition is also an effective way to modify the grade. The samples which has higher molecular weights perform better. For lower molecular weights, the ductility of the system is better.

Similar to Polypropylene, PE also belongs to the group of polyolefin. As their structure are similar, the result may help us understand PCR-PP's behavior. The figure represent that the grade of PE also decide both the elastic and plastic behavior of the material. As expected,

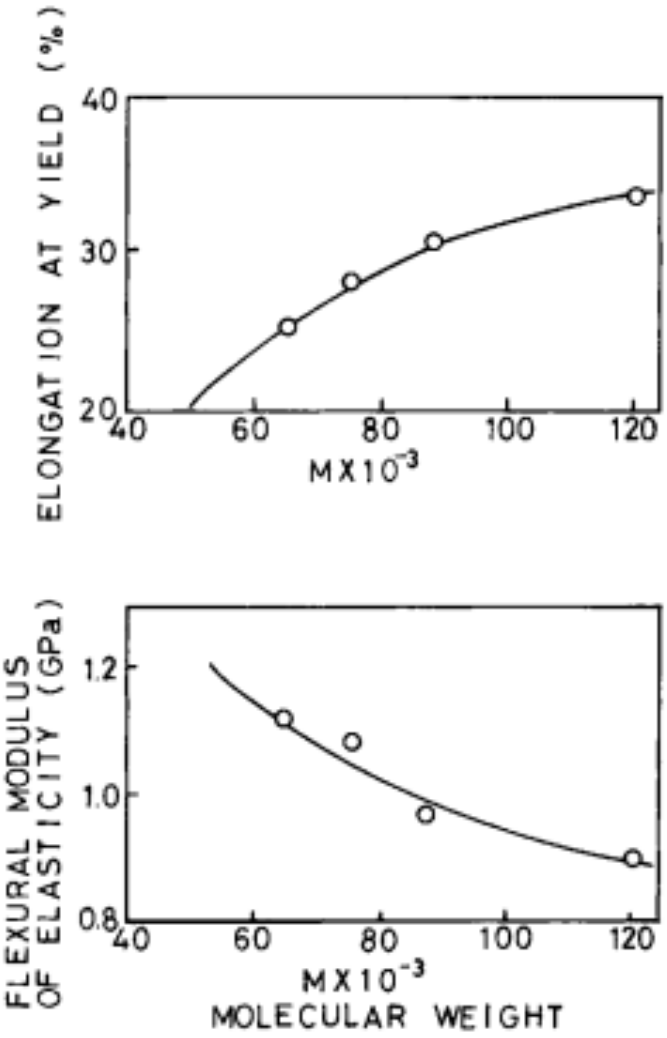

Figure 1.11: Elongation and Flexural modulus of Elasticity [25].

the researchers observe that Young's modulus and tensile strengths at yield and break decreased with increasing m-PE content. The MFI of m-PE(the lowest density polyethylene) sample is 5.0 and for HDPE is 0.3.

A reason why grade or molecular weight influence mechanical properties is the correlation with crystallinity. Aurrekoetxea et al. simulate the recycling procedure of PCR-PP by repeatedly studying its injection procedure[28]. They observed that recycled PP exhibits greater crystallisation rate, higher crystallinity and equilibrium melting temperature than those measured for virgin PP. The explanation from them to the result is the mobility of polymer chains are correlated to the molecular weight, the length of chains. It's proved in the test that the increasing molecular weight prevent further folding of the chain, which caused a decreasing crystallinity. the higher elastic modulus and yield stress of the recycled PP are believed to be correlated with higher degree of crystallinity.

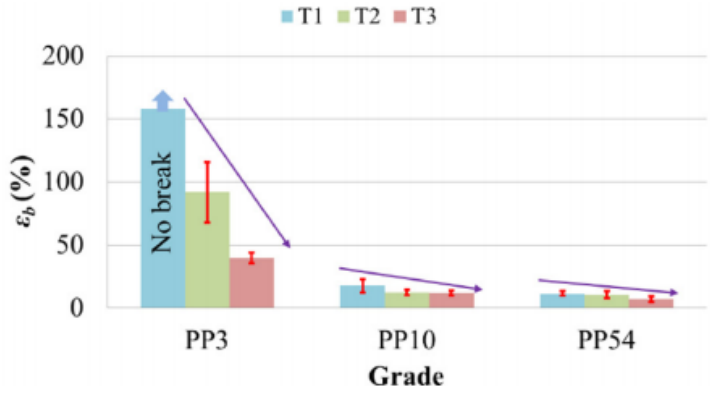

Figure 1.12: strain at break stress for different grade samples[26].

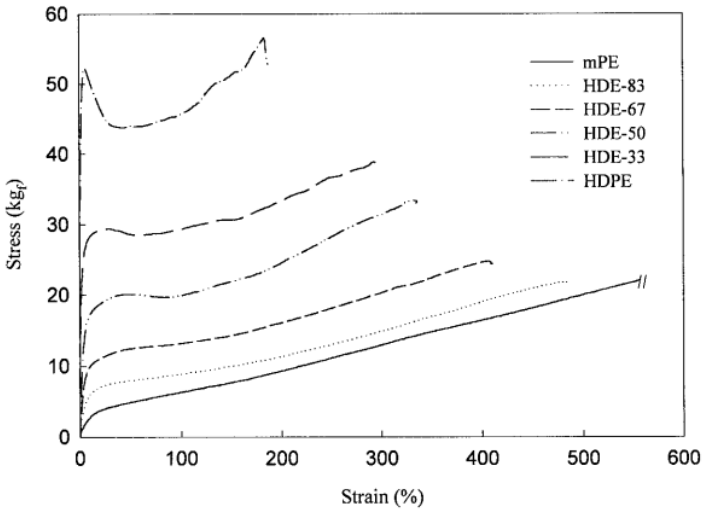

Figure 1.13: :PE grade-stress strain curve.png[27].

TACTICITY

Besides molecular weight, the stereo-regularity of PP also have an effect on the crystallinity. The optical configuration of a polymer refers to the relationship between the group connected to the main chain carbon atom and the reference plane. If the adjacent groups are located on the same side of the reference plane, the polymer is considered to be an isotactic polymer. In a similar way, if two adjacent groups are located on opposite sides of the polymer reference plane, the polymer is considered to be syndiotactic. At present, the artificial synthesis of polymers cannot completely control the formation of the optical configuration of polymers. In fact, identical or syndiotactic structure in the polymer chain segment only exists in a local area. Therefore, we can only use the degree of isotacticity or syndiotacticity to express the configuration of polymers. According to the example in the figure above, this part of the content is displayed as [mmmm] and [rr] defects. mmmm indicates that the side chains on the adjacent four carbon atoms are located in the same plane, so it indicates the degree of isotacticity. rr defects indicate the condition that the neighboring side chains are on the opposite sites.

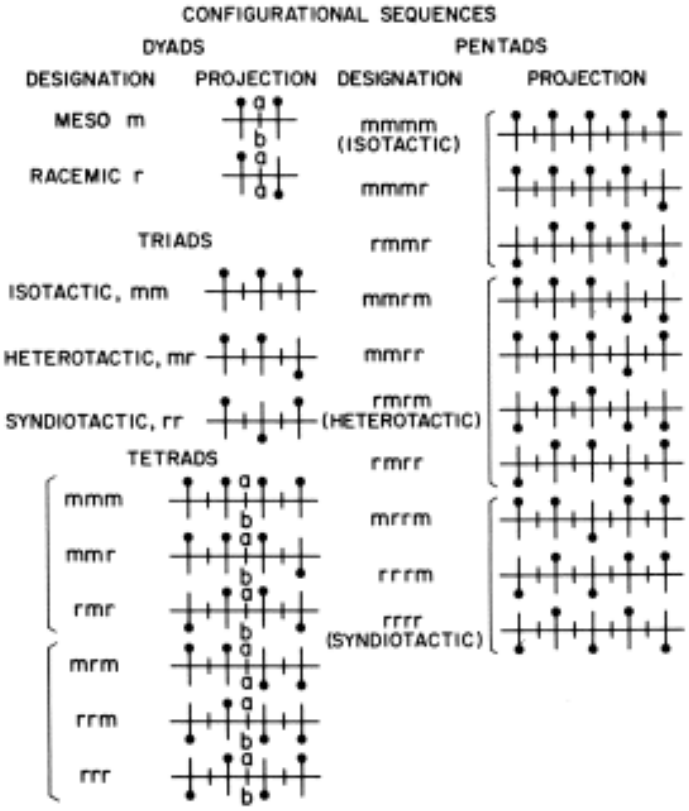

Figure 1.14: configurational sequences[29].

The regularity of the structure is a necessary condition for polymer crystallization, and the regularity includes chemical regularity and three-dimensional structure regularity. Qualitatively speaking, the higher the regularity, the higher the degree of crystallinity that can be achieved[31–34]. Based on the studies of De Rosa, the various stress-strain curve could be measured from different degree of isotacticity samples, which synthesised through designed catalyst [42]. According to the figure, isotactic polypropylene with higher stereoregularity exhibits higher stiffness and yield stress, while polypropylene with higher rr defect concentration exhibits greater elastic limit, which demonstrate the relationship between the crystallinity and mechanical behaviors.

PHASE CONDITION

Phase condition effects the mechanical behavior. The crystalline region of isotactic polypropylene (i-PP) includes the monoclinic alpha form, trigonal beta form, orthorhombic gamma form, and mesomorphic smectic form[18-21]. Under traditional industrial condition, the i-PP products contains mainly alpha form phase. However through various recycling procedure, the phase structure of recycled mixture might change. The thermodynamically stability of the monoclinic alpha form is high at normal conditions and the alpha-phase behaves with relatively good mechanical property[22]. However, the impact strength of alpha phase is poor under low temperature condition. The beta phase exhibits a superior impact performance compared with alpha-PP or amorphous i-PP. Similar to beta phase, gamma phase and mesophase PP are only exist under specific synthesis condition.

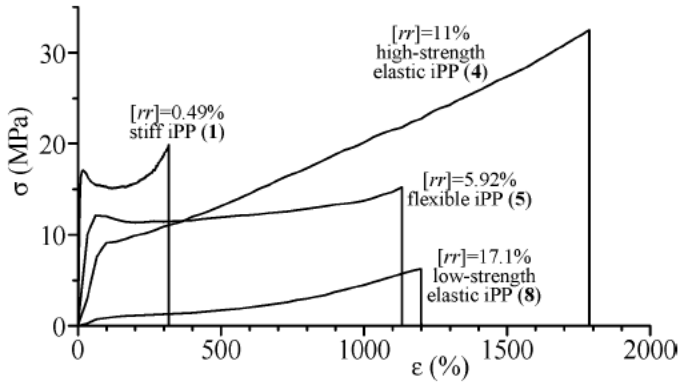

Figure 1.15: Mechanical behavior - tacticity.png[30]

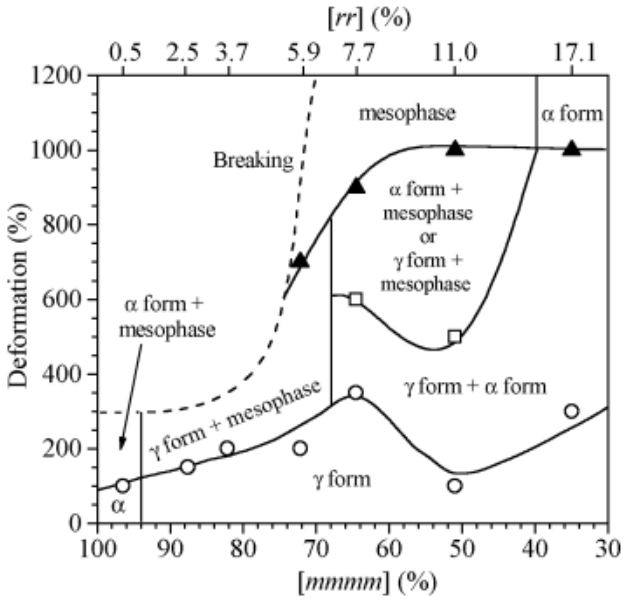

Figure 1.16: phase-tacticity relationship of polypropylene[30].

From the upper figure, the irregularity of molecular chain has an impact on the phase structure of the materials, not only on the crystallinity. With the decrease of PP's tacticity, the equilibrium phase structure changes from gamma to alpha. It could also be regarded as a reason that the stress-strain curve have different shape for various [rr] concentration.

1.3.2. DEGRADATION OF PP

One of the significant environment effects on the recycled plastics is the degradation. The existence of it is inevitable under the effect of cyclic stress and oxygen. Different to the other polymers, the structure of polyolefins is much simpler, so that the degradation does not lead to complex modification on the side chains. The chemical process is detailed in researches[35, 36]

Degradation does not only occur after the polymers are in service. During manufacturing procedures, after the polymerization of polyolefins, the resins are subjected to extrusion. The temperature and shear employed for processing polyolefins lead to the occurrence of

chemical reactions. Even a small degree reaction can have a strong effect on the PP's physical properties. Degradation is able to be initiated by oxygen, shear, heat, catalyst residues or any combination of these factors at any possible condition. The ratio of degraded PP inside the system decides the result of molecular weight and its distribution, as the chains are broken into shorter ones.

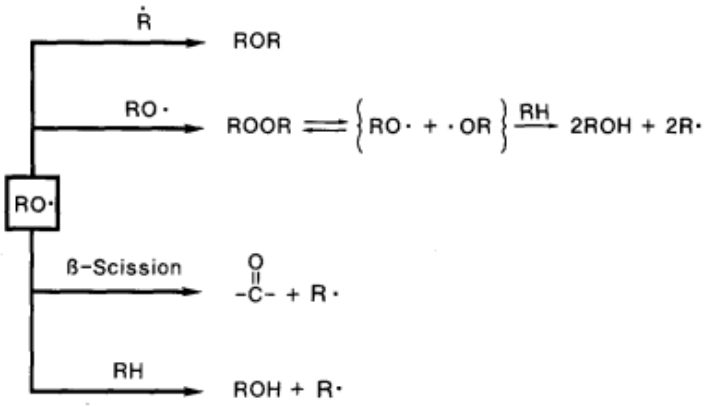

Figure 1.17: Possible Radicals of PP degradation.png[35]

In conclusion, variaty of reasons are summarized to explain mechanical properties differences between virgin PP and recycled PP. The crystallisation changes because of recycling, which might explain the effect on tensile properties. The degradation caused by aging are observed to lead a decreasing impact properties.

1.4. THE CLOSURE MANUFACTURING

Plastics could be divided into two groups which are thermoplastic and thermoset. The majority of plastics are thermoplastic, meaning that once the plastic is formed it can be heated and reformed repeatedly. This property allows for easy processing and facilitates recycling. The other group, the thermoset, can not be remelted. Once these plastics are formed, reheating will cause the material to decompose rather than melt. Plastics can be molded into bottles or components of cars, such as dashboards and fenders. Some plastics stretch and are very flexible. Other plastics, such as polystyrene and polyurethane, can be foamed. Plastics are materials with a seemingly limitless range of characteristics and they have many inherent properties that can be further enhanced by a wide range of additives to broaden their application.

Closures are devices which designed to seal containers. Plastic closures are either thermoplastic - produced via injection molding, or thermoset produced via compression molding.

1.4.1. INJECTION MOLDED CLOSURES

Injection moulding is a common manufacturing technique to produce parts through injecting the molten materials into a prepared mould. Injection moulding is applied in numerous of materials mainly including metals, glasses, elastomers, confections, and most

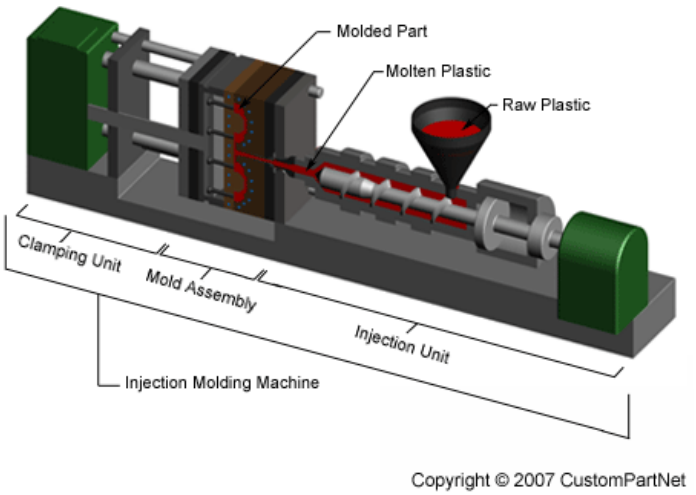

Figure 1.18: Injection Molding Overview[37].

commonly thermoplastic and thermoset polymers. Material is fed into a heated barrel, mixed (using a helical screw), and injected into a mould cavity, where it cools and hardens to the configuration of the cavity. After a product is designed, usually by an industrial designer or an engineer, moulds are made by a mould-maker from metal, usually either steel or aluminium, and precision-machined to form the features of the desired part. Injection moulding is widely used for manufacturing a variety of parts, from the smallest components to entire body panels of cars. Advances in 3D printing technology, using photopolymers that do not melt during the injection moulding of some lower-temperature thermoplastics, can be used for some simple injection moulds.

The injection molding process mainly includes 6 stages: mold clamping, filling, pressure holding, cooling, mold opening, demolding. These 6 stages directly determine the molding quality of the product, and these 6 stages are a complete continuous process. The process conditions include temperature, pressure and corresponding action time that affect plasticization, flow and cooling. Among these parameters, temperature and cooling speed are the key to improve the product quality.The temperature that needs to be controlled in the injection molding process includes barrel temperature, nozzle temperature, and mold temperature. The first two temperatures mainly affect the plasticization and flow of the plastic, while the latter temperature mainly affects the flow and cooling of the plastic.

Through Injection molded methods, the manufactures produce thermoplastic closure primarily from polypropylene, polyethylene or styrene. These closures are designed to be stable and economical. Injection molded closures can be divided into two groups: unscrewing and strip molded caps[38].

1.4.2. COMPRESSION MOLDED CLOSURES

Compression molding is a high-volume, high-pressure method suitable for molding complex, high-strength fiberglass reinforcements. Advanced composite thermoplastics can also be compression molded with unidirectional tapes, woven fabrics, randomly oriented

fiber mat or chopped strand. The advantage of compression molding is its ability to mold large, fairly intricate parts[39].The four main parameters of the compression molding process are the amount of material, heating time, stress applied to the mold and cooling time.

Compression molded thermoset closures are produced from phenolic in dark colors or urea in light colors. These closures are extremely hard and offer excellent dimensional stability and chemical resistance. Compression molded closures are stable at elevated temperatures and are used for auto-claving when combined with a suitable lining material. The processing object can also be vacuum metallized in silver or gold with superior adhesion qualities. Compression molded closures are in general heavier and significantly more expensive than injection molded closures.

In conclusion, it's suitable to manufacture PP closures through injection molding process, to control temperature and cooling speed precisely is essential to enhance the properties.

1.5. SIMULATION OF RECYCLED POLYPROPYLENE STRUCTURES

To produce reliable products from recycled PP, it's essential to predict its behaviors. In the thesis, the performance prediction of closures will be discussed emphatically. For a successful closure product, the following factors are particularly important: (1) ductility, is that, it can work normally under external force without breaking, (2) fatigue resistance. For recycled materials, the fatigue fracture is the main failure situation. According to the fact, it's necessary to establish a model to predict the behavior of products based on several basis mechanical test, then manufactures can fix the design for enhancing the structure. In the case of PCR-PP, one needs to be able to predict its behavior and its reliability when using it as a closure.

The application of FEM aims to replace traditional industrial experiments. Through the comparison of the following aspects, the pros and cons of the two methods are listed. For both of methods, to improve the products quality, engineers need to design a complete test procedure, which include the product improvement direction, parameter changes and the data necessary to interpret the results. In the case of industrial experiments, the real products are required in the experiments, so the real materials, energy cost and a test system would be considered. The advantage of using simulation is that as the data is output from the instrument, so the errors only consist of experimental error. However, on the one hand, the cost of materials and energy will lead to higher product iteration costs, and batch testing of different parameters will greatly increase the time spent for design. Therefore, although this process is more reliable, it is not conducive to improving production efficiency, and it is not an environmentally friendly test method. As for the simulation based on FEM, in principle it can be used to evaluation for more products and designs but the availability of predictions depends on the proper constitutive model which is suitable for the material, and on the availability of adaption to computational resources. Note that FEM does not eliminated experimental testing. The validation of simulation is actually based on the experiments, so its more Eco-friendly. To combine these two methods properly should significantly improve the efficiency of industrial design progress.

1.5.1. FINITE ELEMENT ANALYSIS

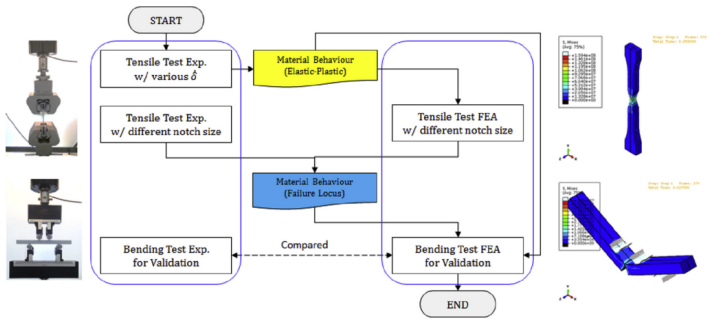

Figure 1.19: general outline of a FEA study on polymer properties[49]

The finite element method is a numerical solution method for elasticity problems. In the early 1950s, it was first applied in the field of continuum mechanics-the analysis of the static and dynamic characteristics of aircraft structures to obtain the deformation, stress, natural frequency and mode shape of the structure. Due to the effectiveness of this method, the application of the finite element method has been extended from linear problems to nonlinear problems. The object of analysis has expanded from elastic materials to plastic, viscoelastic, viscoplastic damage and crack propagation. For this investigation, identifying a good constitutive model for virgin and PCR-PP is the most important task.

1.5.2. POLYMER CONSTITUTIVE MODELS

In general, for the mechanical properties of semi-crystalline polymers, influencing factors include stress state, strain rate and temperature. These three factors make the prediction results inaccurate. In order to accurately match the experimental results, researchers have constructed models with different levels of complexity to predict the viscoelasticity and viscoplasticity of polymer materials. So to reduce the inaccuracies, the models need to take strain hardening and thermal softening into account.

Haward and Thackey first introduced the two branched model to predict the polymeric behavior with the consideration of strain hardening [40]. Some researchers focused on generalizing the uni-axial model into a multiaxial one. Bardenhagen establish a 3-dimensional constitutive model to predict the viscoplastic behavior of polymeric materials [41]. They validated their model with experimental data, and concluded that for modeling polymer materials under various loading conditions. The accuracy of their model is not sufficient.

Thermal softening also needs to be considered to set a constitutive model of polymers. During plastic deformation, mechanical work will transform into heat inside polymeric structures. Boyce's work has shown that the convertion ratio of mechanical work could reach 80%[40]. The ratio for cross-linked polyethylene and HDPE is even higher. Such large amount of heat would lead to the heat hardening which should not be ignored.

1.5.3. INTRODUCTION TO JOHNSEN'S MODEL

To extend the accuracy and reliability of the simulation, a proper viscoplasticity model are required to replace the participant of the simple elastic behavior of Polypropylene.

In the case of polypropylene, we choose the constitutive model published by Johnsen et al. [42] to predict the viscoplasticity behavior. The figure 1.20 shows the general outline of the model.

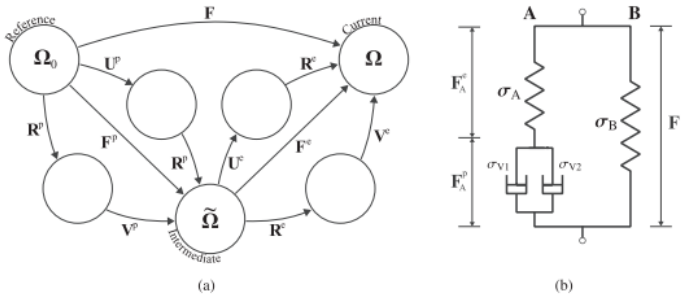

Figure 1.20: (a) Large deformation kinetics of the Johnsen's model (b) rheological model

The multiplicative splitting of the deformation gradient tensor F is used to separate the elastic and the plastic deformation. The unreformed element is mapped from unloaded configuration to the intermediate plastic deformed configuration, and finally to the elastic-plastic deformed configuration. The process is transformed into a matrix expression as the following equation.

$$\mathbf{F}=\mathbf{F}^{e}\mathbf{F}^{p} \tag{1.1}$$

In Johnsen's Model, the total response of the material is divided into two branches, including the branch of inter-molecular properties (branch A), which contributes the viscoplastic and hyperelastic behavior, and the branch of orientational hardening (branch B), which based on the networks' alignment. As two branches share the same deformation gradient

$$\mathbf{F}_{A} = \mathbf{F}^{e}\mathbf{F}^{p} = \mathbf{F}_{B} \tag{1.2}$$

The result of polar decomposition of the elastic and plastic parts of the deformation gradient of Part A shows

$$\mathbf{F}^{e}_{A} = \mathbf{V}^{e}_{A}\,\mathbf{R}^{e}_{A} = \mathbf{R}^{e}_{A}\,\mathbf{U}^{e}_{A} \tag{1.3}$$

$$\mathbf{F}^{p}_{A} = \mathbf{V}^{p}_{A}\,\mathbf{R}^{p}_{A} = \mathbf{R}^{p}_{A}\,\mathbf{U}^{p}_{A} \tag{1.4}$$

Here R stands for the rotation tensor and U and V are right and left stretch tensor, respectively. In view of the fact that this deformation process is defaulted to be an equal volume process, the isochoric deformation gradient tensor $\bar{\mathbf{F}}$ equals to:

$$\bar{\mathbf{F}} = \mathrm{J}^{-1/3}\mathbf{F} \tag{1.5}$$

J is the Jacobian determinant, defined as determinant value of the tensor,thus $\det(\bar{F}) = 1$. The isochoric left Cauchy-Green deformation tensor $\bar{B}$ and the isochoric left stretch tensor $\bar{V}$ are the expressions:

$$\bar{\mathbf{B}} = \bar{\mathbf{F}}\,\bar{\mathbf{F}}^{\mathrm{T}} = J^{-2/3}\bar{\mathbf{F}}\,\bar{\mathbf{F}}^{\mathrm{T}} = \mathbf{B} \tag{1.6}$$

$$\bar{\mathbf{V}} = \sqrt{\bar{\mathbf{B}}} = \mathrm{J}^{-\mathbf{1/3}}\,\mathbf{V} \tag{1.7}$$

Based on the properties of isochoric deformation, $\mathrm{J}^{\mathrm{p}}_{\mathrm{A}} = 1$.For plastic and elastic deformation, the Jacobian determinant reads $\mathrm{J} = \det(\mathrm{F}) = \mathrm{J}^{\mathrm{p}}_{\mathrm{A}}\mathrm{J}^{\mathrm{e}}_{\mathrm{A}}$, which indicates $\mathrm{J}^{\mathrm{e}}_{\mathrm{A}} = 1$. According to the relationships above, the equations are obtained.

$$\bar{\mathbf{F}}^{\mathrm{e}}_{\mathrm{A}} = \mathrm{J}^{-1/3}\mathbf{F}^{\mathrm{e}}_{\mathrm{A}} \tag{1.8}$$

$$\bar{\mathbf{B}}^{\mathrm{e}}_{\mathrm{A}} = \mathrm{J}^{-2/3}\mathbf{B}^{\mathrm{e}}_{\mathrm{A}} \tag{1.9}$$

$$\bar{\mathbf{V}}^{\mathrm{e}}_{\mathrm{A}} = \mathrm{J}^{-1/3}\mathbf{V}^{\mathrm{e}}_{\mathrm{A}} \tag{1.10}$$

$$\bar{\mathbf{F}}^{\mathrm{p}}_{\mathrm{A}} = \mathbf{F}^{\mathrm{p}}_{\mathrm{A}} \tag{1.11}$$

$$\bar{\mathbf{B}}^{\mathrm{p}}_{\mathrm{A}} = \mathbf{B}^{\mathrm{p}}_{\mathrm{A}} \tag{1.12}$$

$$\bar{\mathbf{V}}^{\mathrm{p}}_{\mathrm{A}} = \mathbf{V}^{\mathrm{p}}_{\mathrm{A}} \tag{1.13}$$

1.5.4. INTERMOLECULAR PART

As stated before, the elastic and plastic properties at branch A are regarded as isochoric. According to Hencky free energy, the elastic response is[43]:

$$\rho_0\psi_{\mathrm{A}} = \mu_{\mathrm{A}}(\theta)\,\mathrm{tr}[(\ln(\bar{\mathbf{V}}^{\mathrm{e}}_{\mathrm{A}}))^2] \tag{1.14}$$

ρ_0 here is the initial density of the material, and θ represents the absolute temperature. The temperature dependency of shear modulus is summarized as follows:

$$\mu_{\mathrm{A}}(\theta) = \mu_{\mathrm{A,ref}}\exp\left[-\mathrm{a}_{\mathrm{A}}\left(\theta - \theta_{\mathrm{ref}}\right)\right] \tag{1.15}$$

$\theta_{ref}$is the reference temperature, and the $\mu_{A,ref}$ is the shear modulus at the reference temperature. Based on the equation of energy[44], The Kirchhoff stress tensor is:

$$\tau_{\mathrm{A}} = 2\rho_0\frac{\partial\psi_{\mathrm{A}}}{\partial\mathbf{B}^{\mathrm{e}}_{\mathrm{A}}}\mathbf{B}^{\mathrm{e}}_{\mathrm{A}} = \rho_0\frac{\partial\psi_{\mathrm{A}}}{\partial\ln(\mathbf{V}^{\mathrm{e}}_{\mathrm{A}})} = 2\mu_{\mathrm{A}}(\theta)\ln(\mathbf{V}^{\mathrm{e}}_{\mathrm{A}}) \tag{1.16}$$

The Cauchy stress tensor follows as

$$\sigma_{\mathrm{A}}=\frac{1}{\mathrm{J}}\tau_{\mathrm{A}} \tag{1.17}$$

Then the discussion focuses on the viscoplastic properties. The von Mises equivalent stress are expressed by following equation.

$$\sigma_D^{vm}=\sqrt{\sigma_D^{'}:\sigma_D^{'}} \tag{1.18}$$

$\sigma_D^{'}$is the deviatoric part of the driving stress, σ_D=σ_A.It is essential to be balanced by additional viscous stress related to the Ree-Eyring dashpots[45].

According to the rhelogical model, which is essential here is that the equivalent driving stress of the deformation has to be viscous stress related to the dashpots.

$$\sigma_v=\sigma_{v1}+\sigma_{v2}=\sum_{x=\alpha,\beta}\frac{k_B\theta}{V_x}ar\sin h\left(\frac{\dot{P}}{\dot{P}_{0,x}^{*}}exp\left[\frac{\triangle H_x}{R\theta}\right]\right)=\sigma_D^{vm} \tag{1.19}$$

The alpha and beta represent the main and the secondary relaxation process. V_x stands for the activation volume, $\dot{P}$ is the equivalent plastic strain, and$\triangle H_x$is the activation enthalpy.The deformation-dependent equivalent plastic strain rate, $\dot{P}_{0,x}^{*}$, are obtained through the following equation.

$$\mathrm{P}_{0,\mathrm{x}}^{*}=\mathrm{P}_{0,\mathrm{x}}\exp\left(-\sqrt{\frac{2}{3}}\mathrm{b_x}\parallel\ln(\mathbf{V}_{\mathrm{A}}^{\mathrm{p}})\parallel_2\right) \tag{1.20}$$

$\mathrm{P}_{0,\mathrm{x}}$ equals to the value of $\mathrm{P}_{0,\mathrm{x}}^{*}$ when $\mathbf{V}_{\mathrm{A}}^{\mathrm{p}}=1$, which represent that the system is in the state where is no plastic deformation. b_x controls the deformation dependency. $\parallel\ln(\mathbf{V}_{\mathrm{A}}^{\mathrm{p}})\parallel_2$

The deposition of velocity gradient L_A is given by the following equation.

$$\mathbf{L}_{\mathrm{A}}=\dot{\mathbf{F}}_{\mathrm{A}}+\mathbf{F}_{\mathrm{A}}^{-1}=\mathbf{D}_{\mathrm{A}}^{\mathrm{e}}+\mathbf{W}_{\mathrm{A}}^{\mathrm{e}}+\mathbf{D}_{\mathrm{A}}^{\mathrm{p}}+\mathbf{W}_{\mathrm{A}}^{\mathrm{p}} \tag{1.21}$$

D is the rate of deformation tensor, and **W** is the spin tensor. Then we have the plastic rate of deformation tensor.

$$\mathbf{D}_{\mathrm{A}}^{\mathrm{p}}=\mathbf{L}_{\mathrm{A}}^{\mathrm{p}}=\dot{\lambda}\frac{\partial\mathrm{g}(\sigma_{\mathrm{D}})}{\partial\sigma_{\mathrm{D}}} \tag{1.22}$$

$\dot{\lambda}$ and σ_{D} here stand for a plastic multiplier and plastic potential in turn. If the plastic flow is assumed to be isotropic, the plastic potential is given by

$$g\left(\sigma_{\mathrm{D}}\right)=\sqrt{\frac{3}{2}\sigma_{\mathrm{D}}^{\prime}:\sigma_{\mathrm{D}}^{\prime}}=\sigma_{\mathrm{D}}^{\mathrm{vm}}\geq 0 \tag{1.23}$$

After the inertion of $\dot{\lambda} = \dot{p}$, it is able to obtain the plastic deformation gradient.

$$\dot{\mathbf{F}}_{\mathrm{A}}^{\mathrm{p}} = \dot{\mathrm{p}}(\mathbf{F}_{\mathrm{A}}^{\mathrm{e}})^{-1}\frac{\partial \mathrm{g}(\sigma_{\mathrm{D}})}{\partial \sigma_{\mathrm{D}}} \tag{1.24}$$

1.5.5. ORIENTATIONAL HARDENING

The orientational hardening of polypropylene orinate from the alignment of polymer chains. In Johnsen's model, the chains are modeled through the eight chains model [46]. The entropic free energy is settled based on the research by Miehé [47].

$$\rho_0\psi_B = \frac{\kappa(\theta)}{2}(\ln(J))^2 - 3\kappa(\theta)\alpha\ln(J)(\theta-\theta_0) + \rho_0\psi_T(\theta) + \mu_B(\theta)\lambda_{lock}^2[(\frac{\bar{\lambda}_c}{\lambda_{lock}})\xi + \ln(\frac{\xi}{\sin h\xi})] \tag{1.25}$$

In the part of orientational hardening, the shear modulus is defined as rubbery modulus.

$$\mu_{\mathrm{B}}(\theta) = nk_{\mathrm{B}}\theta = \mu_{\mathrm{B,ref}}\frac{\theta}{\theta_{\mathrm{ref}}} \tag{1.26}$$

n is the chain density in the bulk material, k_{B} is Boltzmann's constant.$\mu_{\mathrm{B,ref}}$ represents the shear modulus at the reference temperature. To standardize the discussion, the reference temperature is usually picked at room temperature, 298.15K, which is also picked in the study. In addition, the bulk modulus would be set as a constant independent to the temperature, and the same for the linear thermal expansion coefficient α. The average chain stretch is given by

$$\bar{\lambda}_{\mathrm{c}} = \sqrt{\mathrm{tr}(\bar{\mathbf{B}})/3} \tag{1.27}$$

ξ is obtained through

$$\xi = \mathscr{L}^{-1}\frac{\bar{\lambda}_c}{\lambda_{lock}} \tag{1.28}$$

$\mathscr{L}$ is the inverse Langevin function, which describe the behavior of rubber-like materials.

The Kirchhoff stress tensor is given by the following equation [48].

$$\boldsymbol{\tau}_B = 2\rho_0\frac{\partial\psi_B}{\partial\mathbf{B}}\mathbf{B} = \frac{\mu_{\mathrm{B}}(\theta)\lambda_{\mathrm{lock}}}{3\bar{\lambda}_{\mathrm{c}}}\mathscr{L}^{-1}(\frac{\bar{\lambda}_{\mathrm{c}}}{\lambda_{lock}})\bar{\mathbf{B}}' + \kappa_{\mathrm{B}}\ln(\mathrm{J}) - 3\kappa_{\mathrm{B}}\,\alpha(\theta-\theta_0) \tag{1.29}$$

here is the second order identity tensor, $\bar{\mathbf{B}}'$ is the deviatoric part of $\bar{\mathbf{B}}$.

Also, the Cauchy-stress tensor is given by

$$\sigma_{\mathrm{B}} = \frac{1}{J}\tau_{\mathrm{B}} \tag{1.30}$$

1.5.6. SELF HEATING AND DISSIPATION

The self heating effect through the mechanical load is considered in the model. The changing rate of free energy and the entropy are given by Miehé [47].

$$\rho_0 \dot{\psi} = \boldsymbol{\tau}_{\mathrm{A}} : \mathbf{D}_{\mathrm{A}}^{\mathrm{e}} + \boldsymbol{\tau}_{\mathrm{B}} : \mathbf{D} - \rho_0 \dot{\theta} s \tag{1.31}$$

$$\rho_0 \theta \dot{s} = -\theta \frac{\partial \boldsymbol{\tau}_{\mathrm{A}}}{\partial \theta} : \mathbf{D}_{\mathrm{A}}^{\mathrm{e}} - \theta \frac{\partial \boldsymbol{\tau}_{\mathrm{B}}}{\partial \theta} : \mathbf{D} + \rho_0 \bar{C}_{\mathrm{v}} \dot{\theta} \tag{1.32}$$

$\bar{C}_{\mathrm{V}}$, the specific heat capacity is given by the following equation. In addition, it is required to be noticed that the specific heat capacity is also related to the deformation.

$$\bar{C}_{\mathrm{v}} = \theta \frac{\partial s}{\partial \theta} = C_{\mathrm{v}} - \frac{1}{\rho_0} \theta a_{\mathrm{A}}^2 \mu_{\mathrm{A}}(\theta) \operatorname{tr}\left[\left(\ln\left(\overline{\mathbf{V}}_{\mathrm{A}}^{\mathrm{e}}\right)\right)^2\right] \tag{1.33}$$

The local deformation power is able to be decomposed into

$$\boldsymbol{\tau} : \mathbf{D} = \boldsymbol{\tau}_{\mathrm{A}} : \left(\mathbf{D}_{\mathrm{A}}^{\mathrm{e}} + \mathbf{D}_{\mathrm{A}}^{\mathrm{p}}\right) + \boldsymbol{\tau}_{\mathrm{B}} : \mathbf{D} = \boldsymbol{\tau}_{\mathrm{A}} : \mathbf{D}_{\mathrm{A}}^{\mathrm{e}} + \boldsymbol{\tau}_{\mathrm{D}} : \mathbf{D}_{\mathrm{A}}^{\mathrm{p}} + \boldsymbol{\tau}_{\mathrm{B}} : \mathbf{D} \tag{1.34}$$

1.6. CONCLUSION

This review, analysis the physical, chemical and crystalline properties of r-PP materials at the level of pure polypropylene, polypropylene co-block polymers and polypropylene mixtures. The physical properties of recycled polypropylene are summarized. The performance of recycled polypropylene is controlled by crystallinity, and its crystallinity is controlled by the length of the polymer chain. Since the length of the polymer chain affects its rheological properties at the same time, we can determine the grade of the polymer chain through rheological experiments and use this as a reference for crystallinity. In addition, isotacticity and other co-polymerization segments will affect the final result of crystallization. The mixture is based on the properties of the interface between polypropylene and other substances, and its mechanical properties are somewhat different from those of pure polypropylene.

A suitable thermo-visco-plastic model is selected to predict the mechanical behavior of polypropylene. The reason why the Johnsen's model is applied here is that it is developed to simulate the mechanical properties of high density polyethylene (PE). As the chain structure of PP is very similar to PE, so its reasonable to use the model in PP's prediction. Till now, there are no literature to discuss whether or not the PCR-PP is available in a over bending structure like active closures for the packaging industry. Therefore, the goal of the thesis is to develop a reliable simulation method which is able to find out the answer.

2

EXPERIMENTS AND SIMULATION METHODS

2.1. DESCRIPTION OF ACTIVE CLOSURES

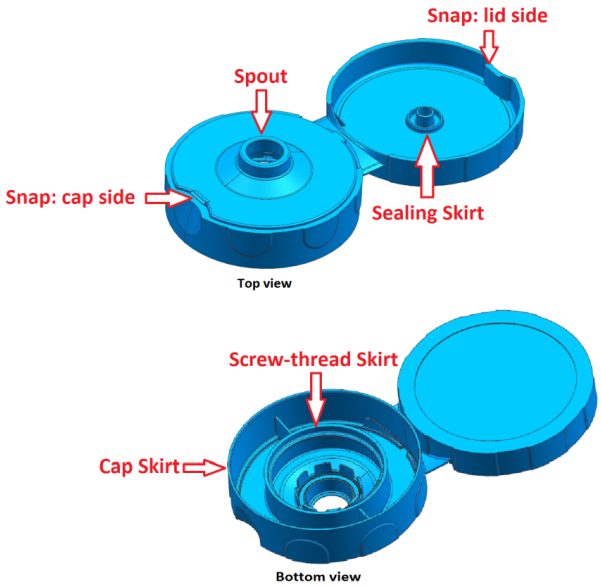

Figure 2.1: Closure overview

Low mechanical properties of PCR-PP has been limiting its aplication in complex loading conditions, . In this project, the focus is on whether or not it is possible to apply PCR-PP in active closures. The goal for the thesis is to develop a finite element model to simulate the deformation of active closures, considering in manufacturing condition and assess if the specific material can be used in them. In the thesis, the closures made by two types of PP, HF840MO and QCP-300P, are discussed in results.The Polypropylene which currently used used in the industrial products of this project (Weener Plastics) is HF840MO. The tensile properties of the PP are shown in the table 2.1. The Young's Modulus of the PP is 1300 MPa. However, the lack of detailed data-sheet made it impossible to to calibrate the viscoplasticity model. So the behavior of HF840MO will only be applied to attempt the boundary

137270 n = 10	E_t MPa	σ_y MPa	ε_y %	σ_m MPa	ε_m %	σ_b MPa	ε_b %	ε_{tb} %	σ_x MPa	b mm	h mm	A_0 mm^2
$\bar{x}$	1301	31,06	10,80	31,06	10,80	21,69	–	505,14	17,63	9,92	3,95	39,175
s	9	0,13	0,09	0,13	0,09	6,36	–	78,84	0,10	0,01	0,00	0,040
V	0,67	0,42	0,82	0,42	0,82	29,31	–	15,61	0,55	0,05	0,12	0,10

Table 2.1: Mechanical Properties of Polypropylene HF840MO

conditions and to see if the linear elastic simulation could foresee the mechanical behavior of closure. Later in chapter-3, the discussion of viscoplasticity is based on the material property of the PCR-PP grade, QCP-300P.

The structure of active closures is shown in figure 2.1. There are two major challenges for PCR-PP to be applied as the base of active closures. The first challenge is that the allowed maximum tensile strain decreases after recycling. This means that the closure might break because of excersi at the hinge middle, or have a shorter lifetime than virgin PP. Meanwhile, even for the virgin PP, if the closures aren't experience the heat treatment that closing it at 69 °C right after the injection molding, it would also break at room temperature. For an injection molded closure, if its cap was opened at original horizontal position without pre-closing before cooling down, it would break at room temperature too. The phenomenon is caused by the residual stress at the hinge. Therefore, the FEM simulation should reflect the necessity of heat treatment during the manufacturing progress.

The manufacturing process could be divided into two significant steps. The first step is right after injection molding. In the processing, through compression provided by the steel cylinder in the machine, the lid is transformed from a horizontally unfolded state of 180 degrees to a closed shape that is just closed. The closure would experience natural cooling down due to convection in the atmosphere, the field temperature at the closure reduced to 25°C. As the closure retains its change during this cool down from 69 °C (342K) to 25 °C(298K), the residual stress at the hinge permanently influences the structural resistance to deformation. In this condition, if customers wish to open the closure, the applied force shall be different compared with higher temperature, as the residual stress remains, and the viscoplastic response of Polypropylene changes at different temperatures. In the thesis, the closing force and the equivalent plastic strain are the key quantities of demonstration.

The other challenge is to predict the snap through angle. The definition of a snap through angle is that after a particular rotation movement of the closure's top cap, there is a specific angle for each active closure's design, where compression force will disappear. The resistance according to the plastic deformation in polymer materials is suppressed due to the buckling effect at the hinge. The observed loose point is defined as the snap through angle. To facilitate a later discussion, the snap through angle is defined as the rotational displacement of the lid. When the closure is closing, the rotation is measured by the angle between the horizontal plain and the lid, and in the case of opening, the rotation is defined as the angle between the bottom of the closure and the lid.

The mechanical behavior of HF840MO closures is tested through a uniaxial compression test. The closure is fixed through the screw-thread skirt perpendicular to the horizontal direction. The direction of the compression force is limited in the y-direction. Through the progress, a set of compression forces at the top of the pressure rod is captured. When snap-through behavior happens, the reaction force will reduce to 0, and the contact between two surfaces disappears. The experiment's basis is to simulate the progress of using hands to close. The test results show the maximum reaction force y-y in a set of compression tests, which is useful for us to calibrate the simulation result. Also, the snap through angle and the closing rest angle at 25 °C is recorded in the table.

Cap	Practice: snap-through	Simulation: snap-through	Practice: Close rest	Simulation: Close rest
Rev.08	130°	130°	165°	175°

Figure 2.2: uniaxial compression test on the closure

2.2. SIMULATION METHOD EVALUATION IN ELASTICALLY RANGE

There exists various options to close the closure. For example, a steel cylinder applies pressure on the cap's top in manufacturing progress, where the following rotation is observed through 180 degrees. After producing, when customers use the products at room

	1	2	3	4	5	6	7
Max Reaction Force y-y (N)	**0.8**	**0.8**	**0.6**	**0.6**	**0.6**	**0.8**	**0.6**
	8	**9**	**10**	**max**	**min**	**avg**	
Max Reaction Force y-y (N)	**0.6**	**0.8**	**0.6**	**0.8**	**0.6**	**0.68**	

Table 2.2: Reaction Force Values in uniaxial compression test

temperature (298 K), the phenomenon is also observed. As the modified loading condition introduces deviation to the simulation result, we will discuss the development under specific assumptions.

As mentioned in chapter 1, Polypropylene is a semi-crystalline polymer material in a wide temperature range. The viscoplasticity behavior of Polypropylene closures increase the simulation cost. Different to viscoplasticity, linear relationship between stress and strain are calculated with higher efficiency and also allow us to utilize the same boundary condition and settings before formal simulation. To shorten the time of developing the FEM model, its reasonable to test boundary conditions considering on elasticity conditions model for PP before considering the comoputationally coostly thermo-plastic model.

The two major branch of general finite element analysis is the explicit dynamic simulation and the static general simulation. Explicit dynamic simulation is used for the instantaneous analysis of the model under dynamic conditions and the analysis of highly discontinuous time. The static general is used to deal with static analysis under linear or nonlinear conditions, without considering inertia and time-dependent material properties.

2.2.1. MESH QUALITY

The mesh quality is important to both explicit dynamic simulation and static general simulation, A coarse mesh would lead to local stress concentration which are not realistic compared with the mechanical test.

Given the challenges of simulating snap through in thermo-plastic structures, a careful meshing strategy has to be followed, suitable for the division of very complex model areas. Because the closure part during this simulation has a morphological structure with multiple local curvatures, a free-form meshing technique is be selected as the method of division. Among the 3D models, the tetrahedral elements are the only structural unit allowed to be used.

The seed distribution, mesh control parameters and element type are key points to mesh a part properly. These three parameters directly determine the mesh quality of the 3D solid model. First of all, the most important determinant is the grid density, which coordinates the calculation accuracy and efficiency at the same time. In the model, in order to improve the calculation efficiency, since the mesh is only used for comparison dynamics display simulation and static general simulation, a relatively sparse seed distribution is applied to obtain larger volume second-order tetrahedral mesh elements. Under current condition, the local seed spacing of hinge is 0.8mm.

The stiffness matrix of the three-bar articulated structure is positive definite, while the stiffness matrix of the four-bar articulated structure is positive semi-definite. It is called as the principle of stability of triangles. The above characteristics are based on the first-order tetrahedral mesh. A.O. Cifuentes and A. Kalbag studied the characteristics of primary and secondary tetrahedrons and hexahedral elements in different structural problems[49]. These structural problems include bending, deflection, torsion and axial deformation. It is observed that the analysis using quadratic tetrahedral and hexahedral elements is equivalent in solution accuracy and CPU time. But it is worth noting that due to the many limitations of automatic hexahedron division, semi-automatic use will consume a lot of time, so the use of quadratic tetrahedron is often the best choice.

By comparing the different results of static general simulation between a mesh of 0.8 mm seed distance and a refined mesh, the loss in accuracy is very clear. The contact force of 0.8mm seeds has the maximum value of 80N, while the refined mesh is 0.3N. In the experiments, the contact force in y direction is measured in the range 0.6-1.0 N, while the maximum reaction force y-y in the simulation owns the value around 60 N. Except for the deviation of elasticity compared with the actual viscoplastic material performance, in the later chapter, it can be seen that the equivalent plastic strain at hinge middle is 80%, and the yield strain is about 40% at room temperature. It's reasonable to expect that for elastic simulation, the measured reaction force is in the range under 2 times higher than the experimental data. So it is illogical that the value of the force differs by two orders of magnitude. The fact shows the importance to have a better mesh. The reason why coarse mesh has a unreal result is that the hinge middle has only one layer of elements, and tetrahedral elements are stable structure which is hard for bending. Also, there exist a shift of snap through point, which is 107° in coarse mesh and 112° in refined mesh. Which means the observed snap through kinetics are also different.

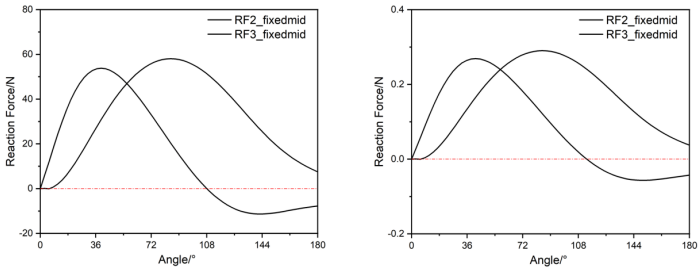

Figure 2.3: Reaction force comparision (left) coarsed mesh (right) refined mesh.

In the refined mesh simulation, the same elastic polypropylene with Young's modulus 1250 MPa is considered.

The refined mesh shows in the figure 2.4. The seed distance decrease from 0.8mm to 0.1mm at the hinge middle, in order to allow the existence of three layers element. The second-order tetrahedral elements are applied in the mesh. To reduce the calculation pressure to the computer, the rest of body remains at 0.8mm. The transition layer between two different density meshes is particularly important, because if the density transition is too

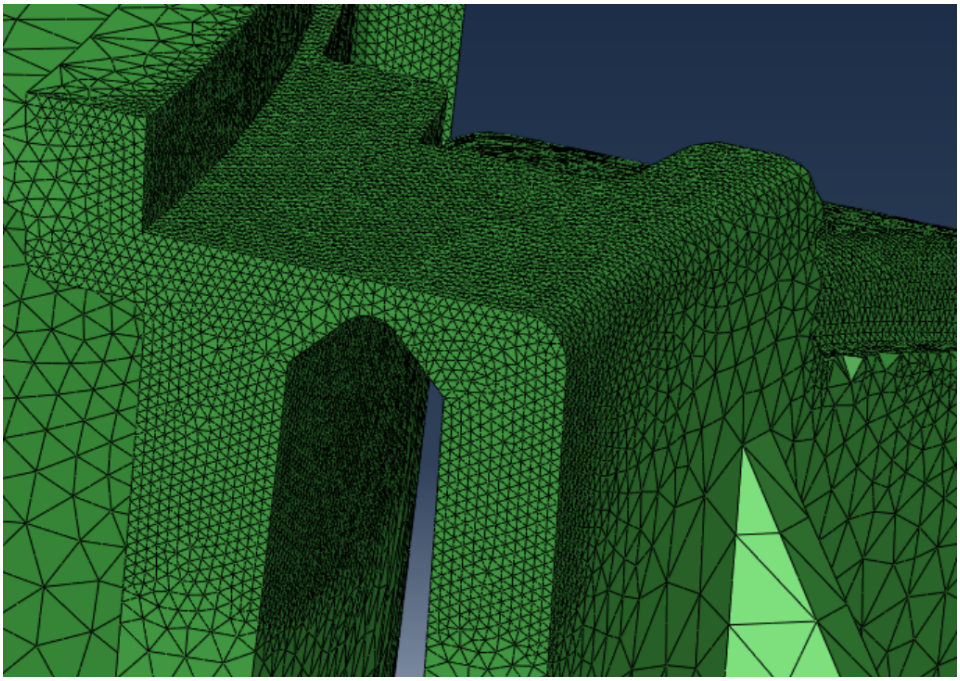

Figure 2.4: local refined mesh

large, there will be sharp triangles in the tetrahedral elements, which will lead to infinite amounts in the analysis process, thereby making the analysis results meaningless. However, there is a complex arc curve at the central turning point of the hinge, so the strategy is to first cut into nearly regular geometric bodies of similar size, and then set up a transition layer between the block and the hinge, gradually transitioning from 0.1mm to 0.2mm, 0.4mm, 0.6 mm, the final transition is 0.8mm mesh element. The final calculation results are shown in the figure below, which uses the same elastic material parameters. The force is reduced to an acceptable range.

2.3. EVALUATION OF EXPLICIT DYNAMIC SIMULATION

Dynamic analysis is the most intuitive way to simulate the actual process. In the explicit dynamic analysis, the displacement and velocity are calculated under the premise that the increment is a known value. Therefore, in the explicit dynamic analysis, the overall mass matrix and stiffness matrix are not inverted.

2.3.1. CENTRAL DIFFERENCE METHOD

The central difference method is based on substituting finite difference for the derivation of displacement with respect to time. The first-order derivation of the displacement is used to obtain the velocity, and the second-order derivation of the displacement is used to obtain the acceleration.

To explain the central difference method, a progress to show how the integration of physical properties are transformed into difference equations [50].

$$\dot{u}^N_{(i+\frac{1}{2})} = \dot{u}^N_{(i-\frac{1}{2})} + \frac{\Delta t_{(i+1)} + \Delta t_{(i)}}{2} \ddot{u}^N_{(i)}$$

$$u^N_{(i+1)} = u^N_{(i)} + \Delta t_{(i+1)} \dot{u}^N_{(i+\frac{1}{2})}$$

In the expressions, u^N stands for the degree of freedom. The reason why central difference method is explicit is that all the results in each increment are based on the steps right before instead of the original physical quantity matrix.

2.3.2. PRE-PROCESSING

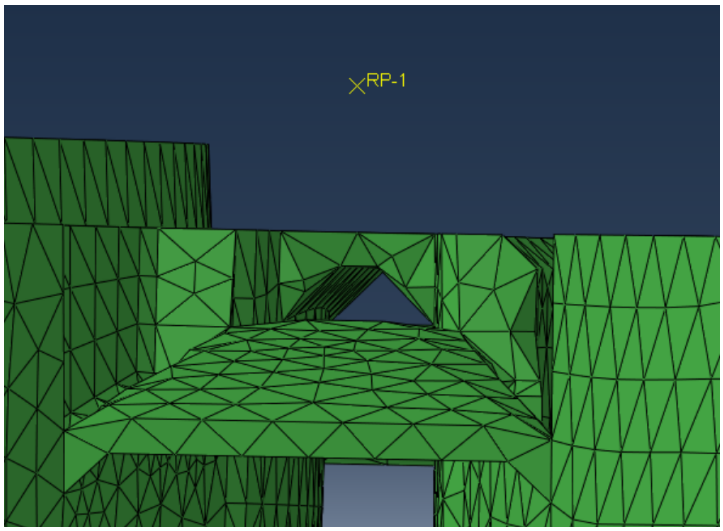

Figure 2.5: Close-up of the coarse mesh used at the hinge midle of the closure

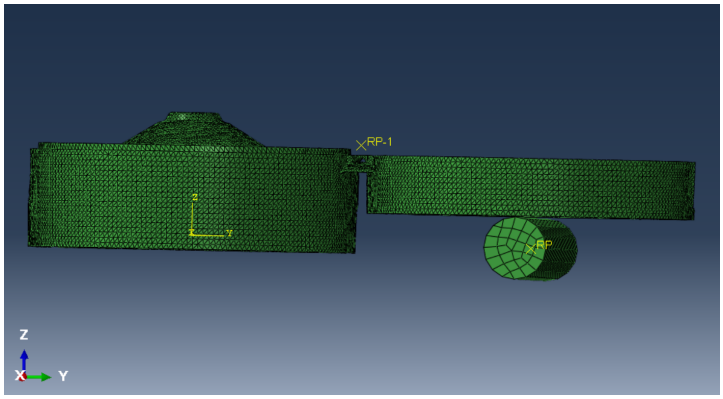

Figure 2.6: Assembly in explicit dynamic simulation

The load isn the explicit dynamic simulation is applied via a discrete rigid cylinder in the assembly, with 10 mm diameter, 60 mm length. Unfortunately, as the real trajectory of how the rigid cylinder used in the mold moves is not available. Therefore, this cylinder in the simulation is assumed to follow a semi-circle trajectory. The assumption of the contact in the simulation for both the self contact and the general contact between cylinder and the lid is a hard, friction less contact to avoid the disturbance from the friction force. To realise

this rotation, the rotation centre is set at 1.5mm higher position than the middle point of the hinge. Both the center of rotation and the inertia of the rigid cylinder are assigned values that are much larger than the mass of the bottle cap to avoid bad contact and mutual interference during rotation.

Based on this, a certain rotational displacement is set on the center of rotation, and the rigid cylinder is controlled to move in the same motion mode through a coupling relationship that locks the six degrees of freedom of motion.The cylinder is set right under the circle centre of closure's lid side. The distance between two parts are 3 mm.

In addition, in order to fix the closure structure, according to the actual process, the inner skirt is set with pinned boundary conditions. The center of rotation only allows rotation around the x-axis.

As mentioned, in a preliminary stays the simulation is to evaluate the feasibility of using an explicit dynamic strategy, the elasticity properties are considered to simplify the simulation. Therefore, no accumulation of plastic strain exists. In this case, the manufacturing-applying progress are equivalent to a same closing step. The rotation step is defined as Dynamic, Explicit, with time period 0.5, which is an estimation of the actual closing time. The geometric non-linearity is considered through the progress, as large displacements happen.

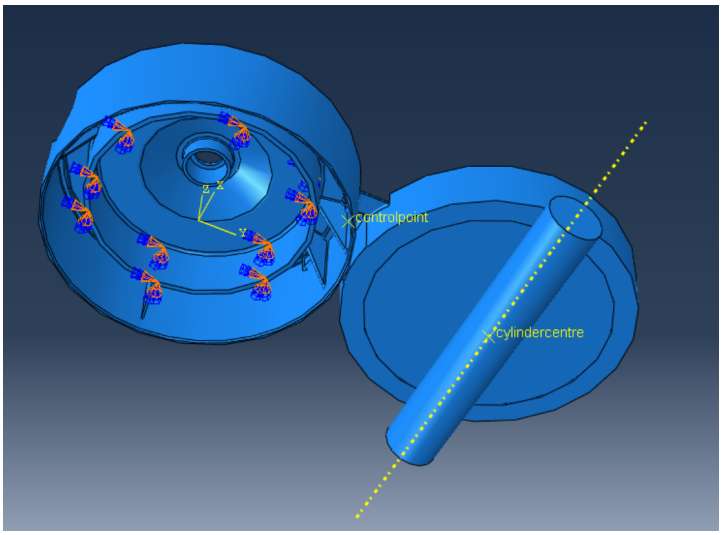

Figure 2.7: boundary condition of the fixed inner skirt in explicit dynamic simulation

2.3.3. RESULT IN EXPLICIT DYNAMIC SIMULATION

Before discussing the specific simulation results, it is necessary to determine whether mass scaling of the model is necessary. The natural time scale plays an important role in dynamic analysis, because an accurate representation of the physical mass and inertia in the model is required to capture the transient response. However, for complex dynamic models, it is common to include some very small elements, which will force Abaqus/Explicit to use a small time increment to integrate the entire model in time. These small el-

ements are usually the result of difficult mesh generation tasks. By artificially increasing the mass of these elements at the beginning of the step, the stable time increment can be significantly increased, while the effect on the overall dynamic behavior of the model may be negligible.

The inaccuracy caused by mass scaling will be directly reflected in the dynamic measurement results. For the contact force, in this simulation, what we are concerned about is the force in the y-axis direction, that is, when the force is positive, the external force object will push the bottle cap to move in the closing direction. When the force is zero, it means that the snap through phenomenon occurs, and the angle that drops to zero will be recorded as the snap through point. Although the strain rate does not affect the stiffness matrix of the material during the simulation of the elastic range, the rotation speed obviously affects the deformation of the closure due to inertial effects. In each test process, a constant rotation time is set as the production process reference value 0.5S, although this is just an estimate.

The approximate value of the stability limit is usually written as the minimum propagation time of the expansion wave through any element in the grid [50].

$$\Delta t \approx \frac{L_{min}}{c_d} \tag{2.1}$$

Here, the maximum stable time increment is Proportional to element size, inversely proportional to dilatational wave speed. The expression of the wave speed is:

$$c_d = \sqrt{\frac{\widehat{\lambda} + 2\widehat{\mu}}{\rho}} \tag{2.2}$$

where ρ is the density of material.

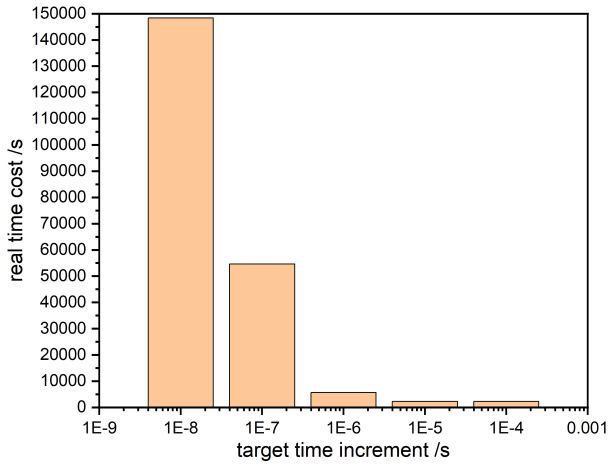

Figure 2.8: Time cost in explicit dynamic simulation

The actual time consumption of explicit dynamic simulations under different mass scaling conditions is counted and compared. Target time increment stands for that if the mass of each element will be scaled until the time increment reach the target value. The result shows that before the increment 1E-7 are reached, the total time cost didn't make much difference on the calculation efficiency, while as the mass are also scale up, the inertial force of the system far more higher then it should be. The kinetic energy will increase due to the extra inertial force. Figure 2.9 shows this increase when the target time increment 1E-6 and 1E-7. At the end of the contact between the cylinder and the closure, i.e. when snap through occur and when the hinge will still undergo a lot of deformation, the kinetic energy grows relative to the elastic potential energy. The smaller the time increment is, the lower kinetic energy is considered in the simulation. In figure 2.10, the kinetic energy is neglectable in the energy distribution. The percentage of increased mass in the simulation (DMass) of 1E-8, 1E-7 and 1E-6 is 3.4%, 8.7% and 25.9%, respectively.

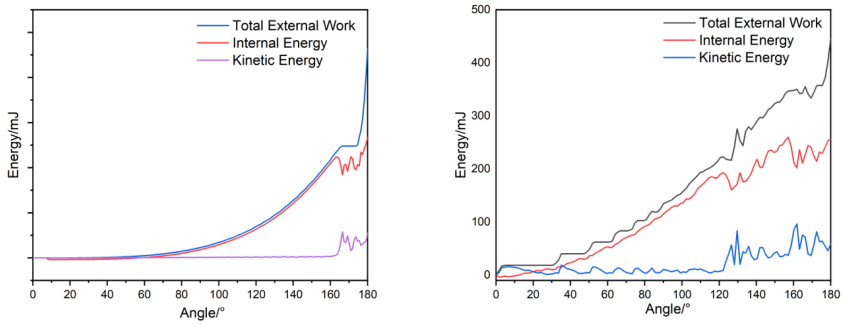

Figure 2.9: energy distribution with target time increment (left)1E-7 (right)1E-6

In the simulation process with the target time increment of 1E-7, the total calculation time of 1E-6 has been increased by about 10 times, corresponding to more accurate calculation results. While the time cost difference between 1E-8 and 1E-7 is about 3 times. By integrating the elements of the contact force in the y-direction of the rigid cylindrical surface, the distribution relationship of the contact force in the y-direction of the system over time can be obtained.

From the model calculation results, we can get a part of valid information for analysis. Including the lateral contact force, and the stress and strain of the hinge position element. After considering a suitable failure model later, stress can be used to predict whether r-PP material can be used as a suitable processing material. Compared with 0.6N in the experimental results, the contact force of 4N is still too large in the results of target time increment 1E-6, which is caused by the existence of inertial force. It's also shown in the energy distribution figure 2.8 that the kinetic energy take a large part in the simulation. As for the results of target time increment 1E-7 and 1E-8, the kinetic energy is relatively low compared to the total external work. By comparing the maximum reaction force with the experimental value, the value of 1E-8 and 1E-7 is acceptable while the result of 1E-6 is relatively too large. As the experiment is carry out in a quasi-static loading condition, its reasonable to expect that inertial effects take a little part in the necessary reaction force. So the result with lower

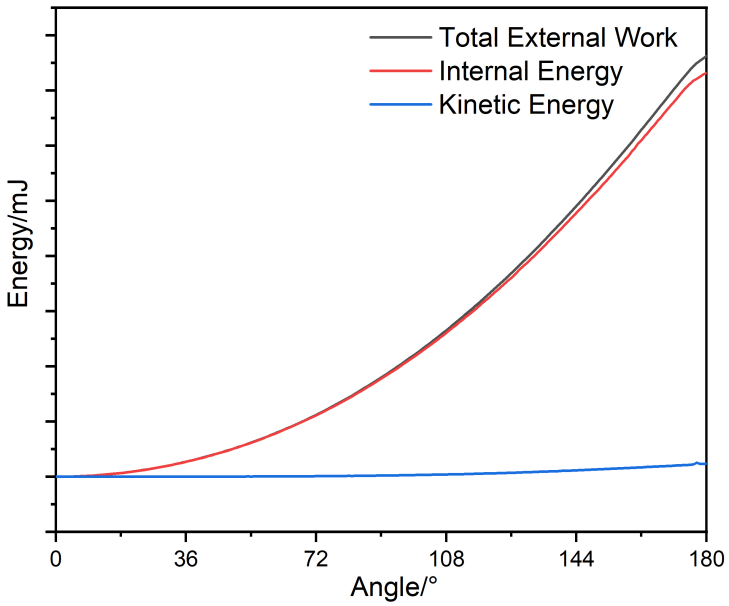

Figure 2.10: energy distribution with target time increment 1E-8

target time increments is more reasonable. Notice that the time cost between 1E-8 and 1E-7 has a large different, and the result of energy distribution and reaction force y-y is similar, there is a tendency that maximum reaction force converge at 1.8 N. The target time increment 1E-7 is better to be applied as it combines with accuracy and efficiency. However, There is no observed intersection between the zero line and the contact force y-y curve, so the snap through point cannot be accurately predicted. When cancel the mass scaling, the job is stop for the reason unknown, so it is not compared here about the result with no mass scaling. Therefore, the application of explicit dynamics simulation is not a good way to predict the mechanical properties of the closure, and it requires for further study. The permanent conclusion is target time increment 1E-7 is a acceptable mass scaling condition to reach the result. By refining the mesh locally or try the accurate loading trajectory might improve the observed reaction force to capture the snap through point in explicit dynamic simulations.

2.4. EVALUATION OF STATIC GENERAL SIMULATION

The core difference between the static analysis process and the dynamic explicit analysis process is that it is a model that does not contain the internal history of previously applied input values, internal variable values, or output values. The important advantage of statics analysis is that it can avoid the effect of inertial force, so as to avoid the division of kinetic energy and viscous dissipation for the total energy in the quasi-static calculation process, to obtain the actual contact force more accurately.

Originally, the equation of motion of the system is:

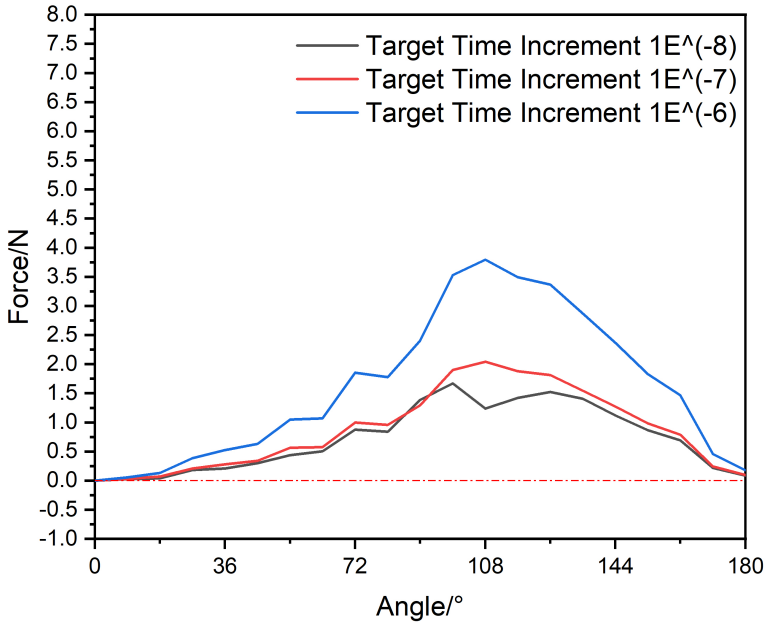

Figure 2.11: Measured reaction force in y direction of different target time increments

P – I = ma

m = Mass Matrix P = External Forces

I = Internal Forces a = Acceleration

v = Velocity u = Displacement

(2.3)

When inertial forces are small (m -> 0), the equation reduces to the static form of equilibrium.

P – I = 0

I = Cv + Ku

C = Damping K = Stiffness

K = EM

E = Elastic Modulus M = Moment of Area

(2.4)

2.4.1. BOUNDARY CONDITIONS

In the dynamic simulations, it is observed that when the simulation runs upon a smaller mass scaling factor, the kinetic energy only takes a low percentage of total system energy and the inertial force is relatively low. And the kinetic energy finally approach 0 when the target time increment is 1E-8, when the inertial force is also converged. So its reasonable to

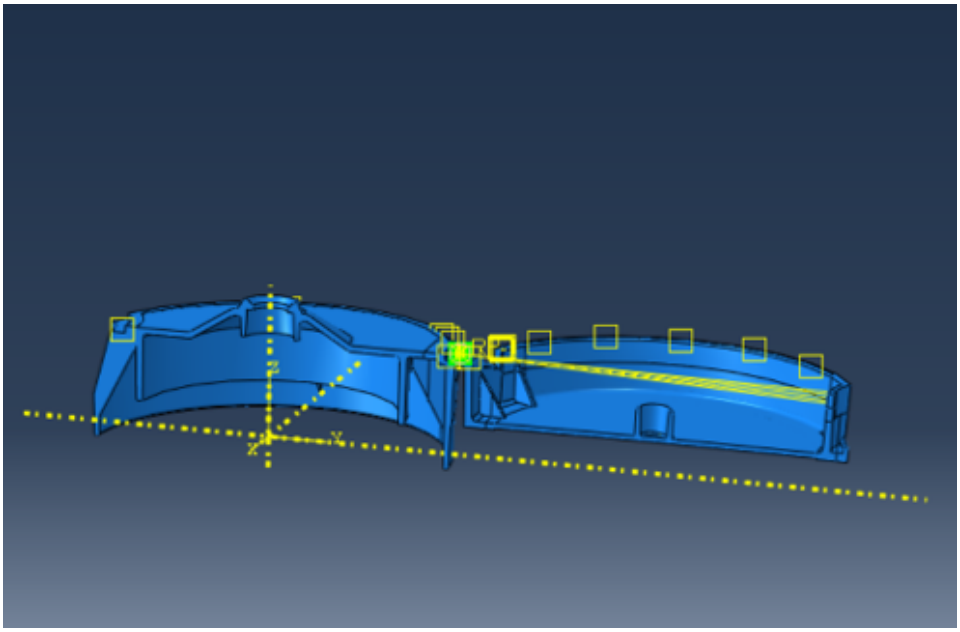

Figure 2.12: boundary condition of the fixed inner static general simulation

assume, that when the mass scaling ratio is very low or 0, which should have the same time scale of the real processing, the total reaction force should include two parts, the first part is the visco-plastic response of the hinge, and the other is a certain value decided by the real density. By test the real processing, the inertial force is able to be calibrated through a set of experiments of different rotational velocity for the same material. After removing the inertial force part, if there is a certain way to predict the viscoplasticity response, it should able to fully predict the processing of closures in PCR-PP. Therefore, the static general strategy is applied to avoid high computational cost of explicit dynamic simulation. and also gains a accurate response base on the constitutive model.

Since there is no need to consider the deformation caused by the collision of the cylinder, the overall closure structure can be simplified to half, which can be achieved through symmetric conditions at y-z middle plane. In this simulation, a small area at the top of the lid is coupled with the middle reference point. This coupling includes six degrees of freedom of motion. This constraint replaces the original cylindrical loading method, and directly drives the coupled area to move according to a specific circular curve through the rotation of the reference point, thereby driving the entire continuum to move. According to the equivalence of structural mechanics, we can think that the lid undergoes the same rotation process, and the force provided by this reference point is equivalent to the contact force of the rigid cylindrical surface, so the output reaction force in the simulation results can be used to predict the force of the lid. In addition, the way of fixing the lid and the reference point is the same as that of the dynamic simulation.

The time increment of static calculation is not limited by the stable time increment. By default, the incremental step size of Abaqus/Explicit in the analysis process is completely controlled by the solver automatically. This control method is called the automatic incremental step method. In each static analysis step, when the deformation of the object is too

large, geometric non-linearity needs to be considered, so the step will be divided into several incremental steps, performing iterative calculations in each incremental step, which involves convergence issues. A large time interval might lead to no convergence.

2.4.2. RESULTS IN STATIC GENERAL SIMULATION

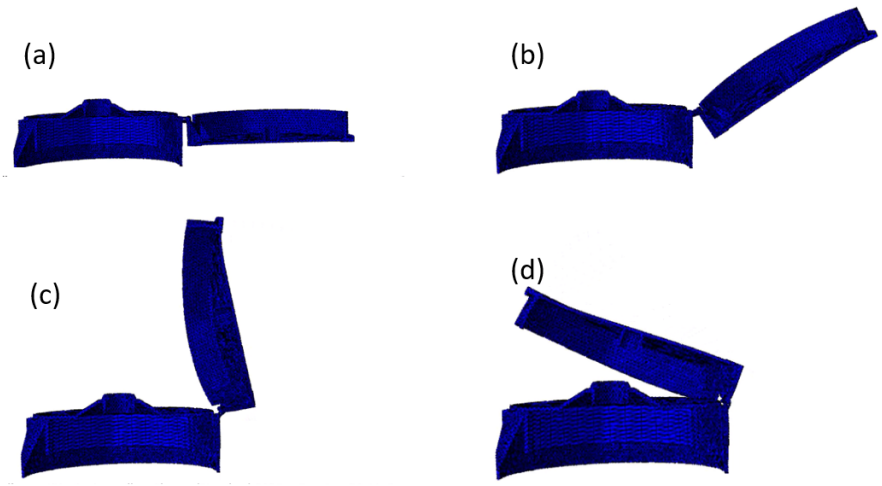

Figure 2.13: distortion progress through static general analysis (a) 0° (b) 30° (c) 90° (d) 150°

In Fig 2.13, a unnatural distortion is observed at the top of cap, which is caused by the coupling. Such a distortion shows the result that the current boundary condition is not working with clean kinetics. In this case, the reaction force is always positive in several simulations, which means the snap through point is not observed under current settings. In order to eliminate this unnatural distortion, we cut the cap into three parts, the hinge in the middle and the supporting structure without hinges on both sides. After the segmentation is completed, the hinge in the middle maintains the original elastic properties, while the sections on both sides are given extremely high stiffness, E=1E6 MPa, which can be approximated as a rigid body. After repairing, the normal rotation process can be observed in fugure 2.14, and the snap through behavior is shown in later results.

In the analysis results, RF2 represents the force component on the y-axis, and RF3 represents the force component on the z-axis of the reference point. To compare the differences between the methods, the reaction force is compared at the top of the coupling or the bottom of the coupling to observe which conclusions the selection of this position will affect. Still, the chosen coupled area at the closure top will influence the result, which is shown in figure 2.15. The fixed top and bot means the top or the bottom of lid's tip is coupled with the reference point.

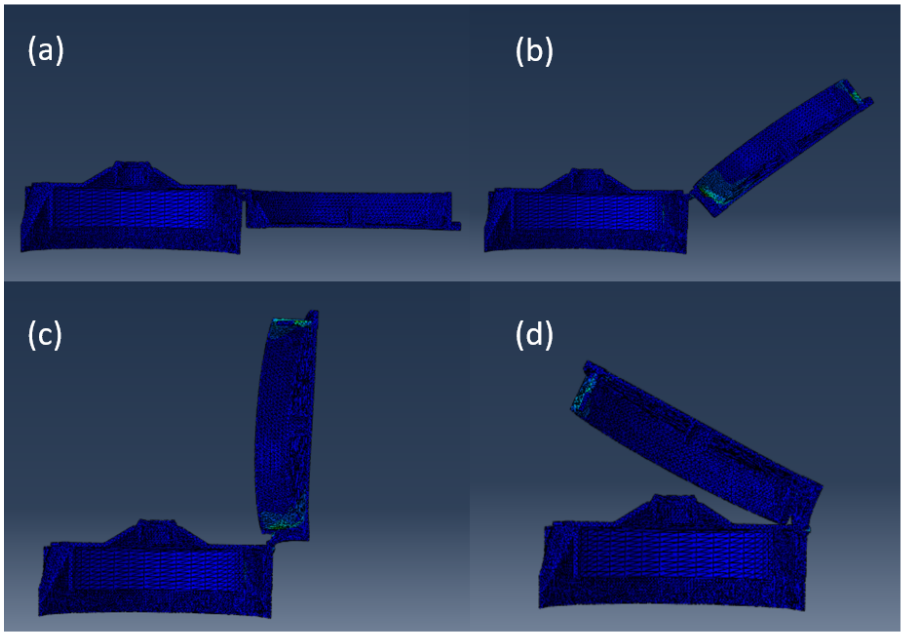

Figure 2.14: rotation progress with rigid body assumption (a) 0° (b) 30° (c) 90° (d) 150°

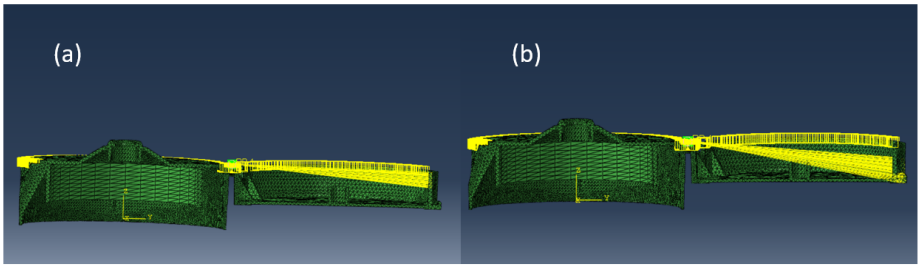

Figure 2.15: Different Coupled part (a) coupled top (b) coupled bottom

According to the analysis results, from both coupling methods, snap through occurs at around 110°, while the component values of the force in the y direction and z direction are significantly different. The closer the coupling position is to the top plane, the smaller the force it is. It shows that various coupling strategy will not leave an observable shift on the snap through point. A reasonable hypothesis to explain why the reaction force amplitude are different is that the projection component of the torque of the bottom coupling on the rotation plane is smaller, so the force consumed is greater.

As the simulation in the elastic range has no accumulated plastic strain and cannot effectively simulate the movement of the bottle cap after high temperature processing, it's still available for us to observe how the temperature effect the rotation performance of the closures. At 69 degree Celsius, the Young's Modulus of HF840MO is down to 230 MPa.

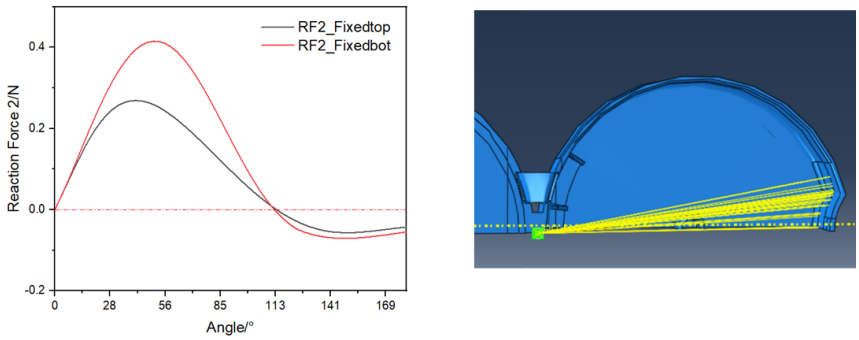

Figure 2.16: (a) Reaction Force curves for various coupling strategy (b) Schematic diagram

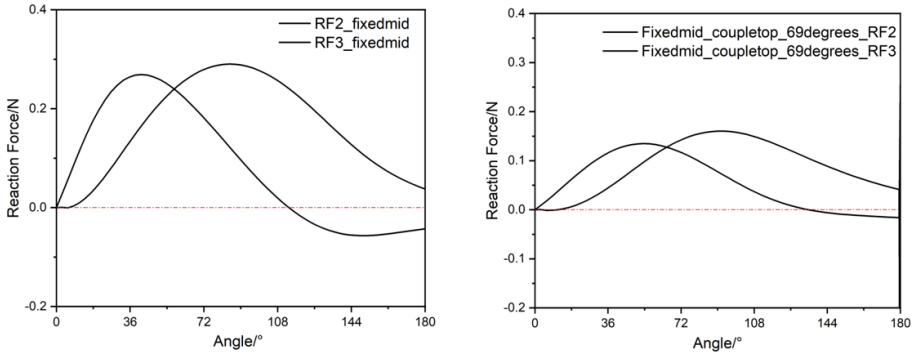

Figure 2.17: Reaction Force on the reference point at room temperature.(left)/69°C (right)

The snap through point is observed later after the temperature rises.Therefore the buckling effect in the plastic body is less likely to occur at higher temperatures. Since the Young's modulus of the material decreases at high temperatures, the two forces also have smaller amplitudes in the elastic analysis. According to the experimental data, the closing snap through happens at 100 degrees under room temperature, which seems to be in good agreement with the experiments.

3

Structural Analysis Based on Viscoplasticity Model

3.1. Results Discussion of Viscoplasticity simulation

This chapter includes the thermoplastic constitutive model in the finite element model. Recall that the manufacturing of closure has 3 stages, the first stage is the closing at 342 K after the injection molding, follow by cooling down and openning at room temperature 298 K.Then the closure is ready to be used at room temperature. Due to computational resource limits,simulation of the complete process with a fine mesh are not possible. So only the first step is simulated with a fine mesh, to show the ability of current model. In the following sections, the discussion will be based on the simulation with a coarse mesh, to capture the tendency of the reaction force which allows a qualitative analysis on snap through behavior.

Thanks to the work of my fellow college Manoj, who calibrated the Johnsen's Model with QCP-300P. The calibration is according to ASTM D638, the test method for tensile properties of plastics. This protocol is carried out on "dog bone" shaped samples, and the tests are under different pre-treatment, temperature and humidity conditions as per the different speeds of the testing machine. In FEM simulations, the dog bone sample is created as a part. The loading is set on one side of the sample, to have a tension with certain strain rate. After get the stress-strain curve of the element at sample's middle, the parameters are fitted to the curve through bayes optimization. The whole step is defined as the calibration. After the calibration, the viscoplasticity model is able to predict the response of the material. The calibrated properties is in table 3.1.

Figure 3.1 shows the FEM prediction with the calibrated thermoplastic model. The maximum reaction force y-y occurs at 45.4°, with value 0.92 N. After the peak, the buckling effect happens due to the bending at the hinge, the reaction force decreases. Snap through angle is observed at 104° at 342K. One significant difference between the result in elastic range and the viscoplasticity model is that the snap through point moved left for about 30°, the elastic snap through happens at 138° and the viscoplastic snap through point at 105°, for the material QCP-300P at 342 K manufacturing condition. The strain hardening in the polypropylene under a certain temperature and strain rate exhibit a significantly lower resistance to the deformation when compared to perfect elastic material.The figure 3.2 shows

position=above

Table 3.1: Calibrated material properties of QCP-300P

	Property	SI Units	Cross-Linked PE
Part A	$\mu_{A,\,\mathrm{ref}}$	MPa	480
	a_A	K^{-1}	0.02
	θ_{ref}	K	298.15
	ΔH_α	kJ/mol	2.48×10^5
	V_α	nm^3	4.17
	$\dot{p}_{0,\alpha}$	s^{-1}	9.92×10^{34}
	b_α	–	1.75
	ΔH_β	kj/mol	2.41×10^5
	V_β	nm^3	3.02
	$\dot{p}_{0,\beta}$	s^{-1}	3.66×10^{36}
	b_β	–	9.99
Part B	$\mu_{B,\,\mathrm{ref}}$	MPa	3.8
	κ_B	MPa	400
	λ_{lock}	–	5

the equivalent plastic strain in the deformation progress in the centre element of the hinge.

The equivalent plastic strain is a physical quantity used to determine the position of the yield surface of the material after strengthening, At the snap through point, the equivalent plastic strain is predicted to be 0.29.

In addition, since the closure is deformed at 342K and then it is cooled, it accumulates a residual plastic strain. Therefore, after cooling, the closure is given a new characteristic which is called open rest angle. Due to the existence of plastic strain, the opened cap does not stay in a horizontal state, but there is a specific tilt angle derived from plastic deformation.

To capture the open rest angle, two additional steps are necessary to be added after the original closing, including the opening at 298 K, and the closing at 298 K. To simplify the simulation, the heat exchange between atmosphere and the closure's surface is not included in the interaction settings. The 0.8mm global size mesh is applied in the simulation, so the following simulations are not accurate. The same material's parameters are applied in the model. So in this case, the goal is to reveal the tendency of shifted snap through point, and the parameter sensitivity.

The figure 3.3 is the reaction force results for both closing and opening process. Different to the black curve corresponding to closing the closure at 342 K, the red curve which describes the opening progress shows a new intersection at 10 degrees. This feature is defined as the opening rest point, the stable angle without external force, where the lid will stay open without further external force. The opening snap through is captured at 100 degrees.

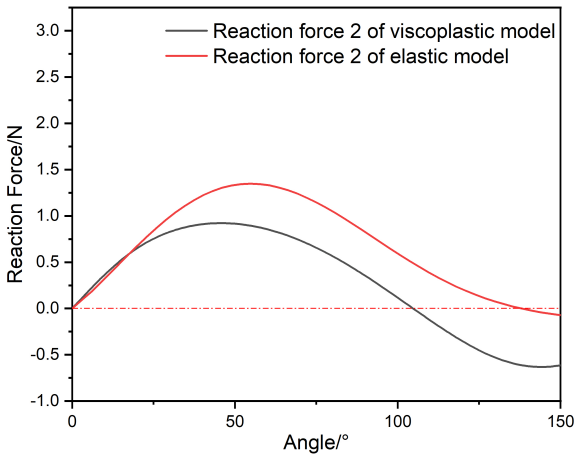

Figure 3.1: The reaction Force y-y in 342K simulation, viscoplastic/elastic properties

As the Young's modulus and the equivalent plastic stress both increase at lower temperature, the peak of opening reaction force y-y is higher than during the closing process.

In figure 3.4, When the closure is closed again at room temperature, the larger snap through angle compared with the original closing at 342K is observed. Based on the accumulated plasticity, the closed rest point is observed at 25 degrees, which is the stable position at which it remains opening. The reaction force value become higher at 298K compares with 342K.

Notice that there exists a diversity between the simulation result and the experiment result. The closing/opening snap through in the experiment is 130/80 degrees, and the closing/opening rest point is 15/5 degrees respectively. However, recall that the experiment was conducted for a different material, i.e. HF840MO instead of QCP-300P. In addition, the mesh used is coarse and the constitutive model has not been carefully calibrated, so its not our main purpose to have a very accurate snap through behavior prediction. constitutive model will also influence the accuracy of results, so its not our main purpose to have a exact same snap through behavior in simulation with the experiment.

3.2. FAILURE CRITERIA OF POLYPROPYLENE

To reveal if the recycled polypropylene is a stable material for the closure, including a failure model of PCR-PP is necessary. As reviewed previously, failure of polypropylene includes degradation, mechanical failure and oxidation. In the study of Wal [51], the fracture behavior of PP is based on the testing condition and also material properties, crystallinity and molecular weight. To simplify the discussion in the thesis, mechanical failure is the only factor considered.

Due to the high simulation cost, the fatigue behavior of the closure is also not discussed in this thesis. We are focusing on the failure at the first opening-closing round after the

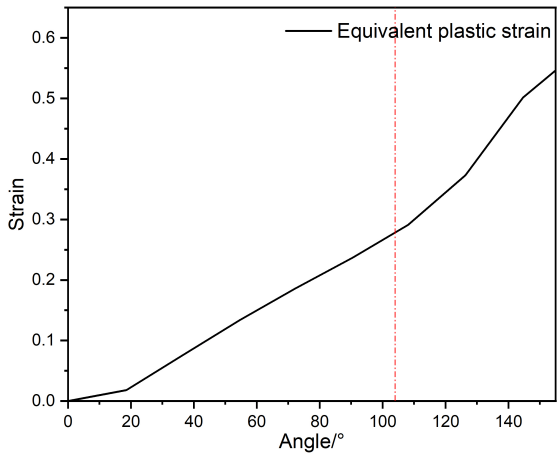

Figure 3.2: equivalent plastic strain at 342K in hinge middle

heat treatment. The maximum deformation happens at the downside of the corner of hinge. The hinge structure is shown in the figure 3.6. According to the simulation result, the equivalent plastic strain for this point during the simulation is already higher than the onset strain of yielding. It's reasonable to discuss about the ductile fracture on the closure. The method here to predict the failure is the maximum strain criterion, due to the ductility of PCR-PP. So the criterion is calibrated by the uniaxial tensile test result of QCP-300P. To prevent failure, the limitation of extension is set at the maximum strain at different temperature.

Through the simulation, the maximum equivalent plastic strain exists at the middle and bottom of the hinge, where it has minimum thickness and undergoes maximum bending. The equivalent plastic strain is shown in the figure 3.5. According to the result, among the rotation at 69°C, the element will need to take 58% equivalent plastic strain. According to the uniaxial tensile test, the plastic strain at that temperature can be much higher until failure. So, the material is not expected to fracture at that temperature.

In the tensile test, the tensile behavior of QCP-300P is tested in two different temperature, including the heat treatment temperature and the room temperature. Recall that the manufacturing process closes the closure right after the injection molding before the cooling down. If the closure didn't experience this, the hinge would break at room temperature when closing it. This phenomenon is also explained in our results.

Under 69°C, The average maximum strain measureed for QCP-300P is 358% . Compared with the simulation, the maximum equivalent plastic strain during closing progress is 58% at 160°, and even at 180° the equivalent plastic strain is significantly lower than the limit. While at 23°C, the average maximum strain is 35.8%, relatively lower than required strain. So the bending at higher temperature works as a strain hardening to the product enable it with higher resistance to breaking according to the maximum strain failure criteria. This

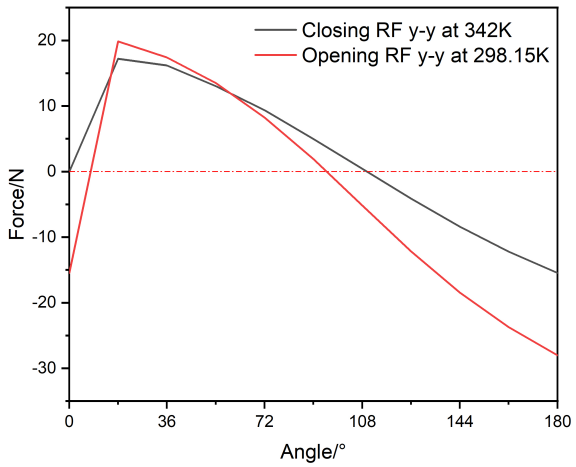

Figure 3.3: The reaction force y-y of opening at 298K, after the original closing at 342K.

results explain the necessity of closing at 342K, so the maximum strain criteria is partly able to explain the behavior of PP.

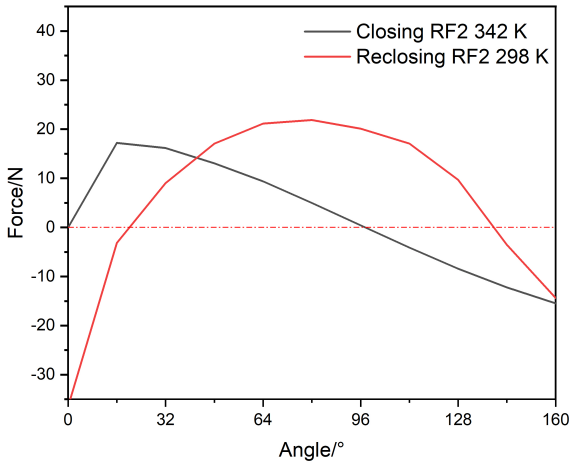

Figure 3.4: Reaction force in re-closing progress

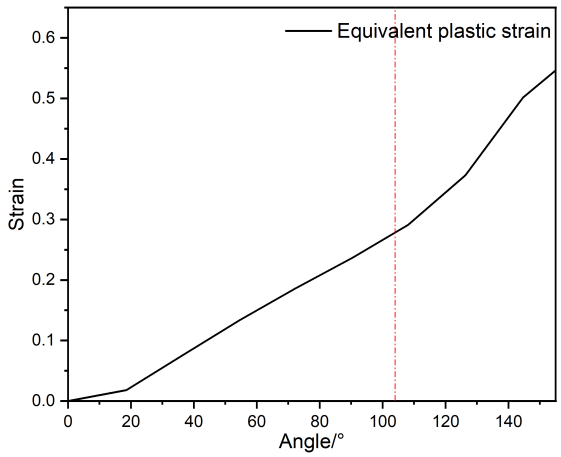

Figure 3.5: equivalent plastic strain at 342K in hinge middle

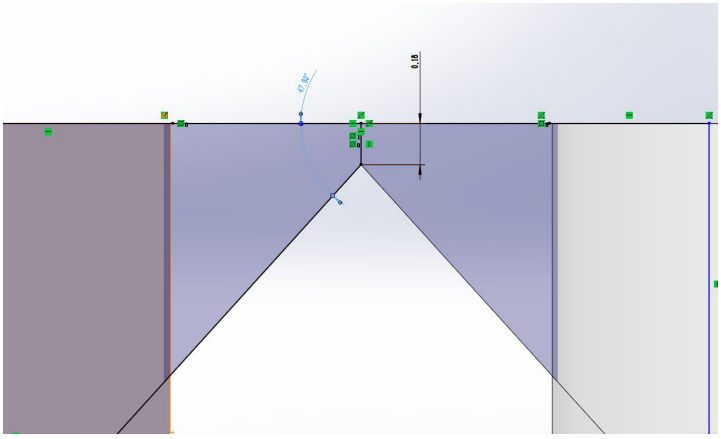

Figure 3.6: Hinge Structure

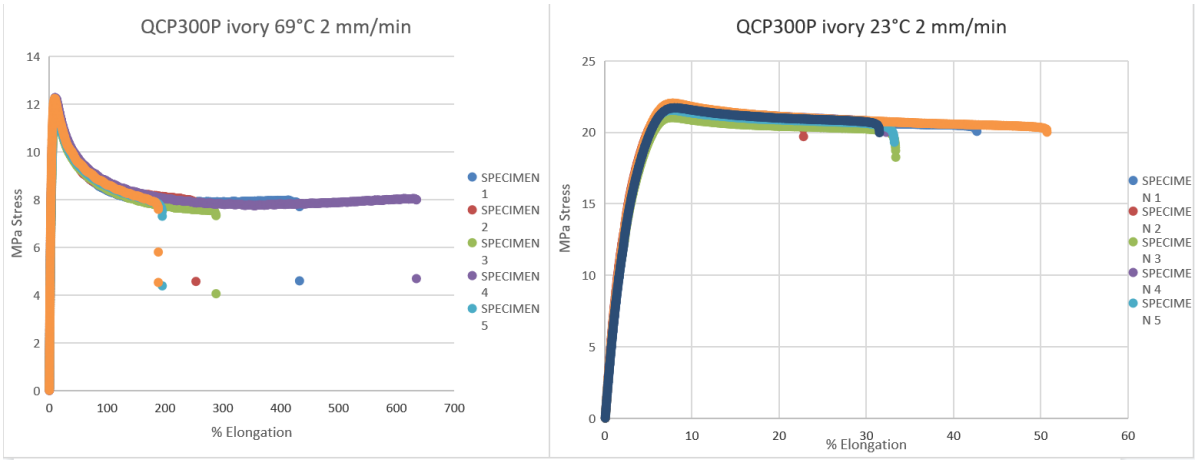

Figure 3.7: Uniaxial tensile results of QCP 300. (a)69°C(b) 23°C

4

CONCLUSION

This thesis is concentrated on simulating the mechanical behavior of PCR-PP active closures. The weakest part of the structure is the hinge, which is corrolated for the snap through behavior and the closing force.Finite element analysis demonstrated that inertial effects may be non-neglectable during the closing process of the closure in the mold after injection molding. These simulations, however, are computationally expensive, Therefore, implicit static finite element analysis was developed to predict the quasi-static closing process and compare it with a simple experimental measurement. These simulations constructed simplified boundary conditions but they showed reasonable agreement with experiments when considering an appropriate thermoplastic model. The model is able to approach the behavior of real closures, predicting the snap through behavior point. A simplified failure analysis was conducted focused on the maximum strain criteria to explain the necessity of closing at high temperature after the injection molding step during manufacturing.

Still, there remains several questions for future study. The finite element model can be improved by using better constitutive models, especially the failure criteria and damage models. These models can be used to predict fatigue behavior. Additional improvements of the boundary conditions would be beneficial. Furthermore, once high-quality simulations are available, it would be interesting to use machine learning methods to design new closures that cause smaller deformations at the hinge.

BIBLIOGRAPHY

[1] *History and future of plastics,* (2019).

[2] http://www.plasticseurope.org.

[3] https://omnexus.specialchem.com/selection-guide/polypropylene-pp-plastic.

[4] H. A. Maddah, *Polypropylene as a promising plastic: A review,* Am. J. Polym. Sci **6**, 1 (2016).

[5] R. R. Tupe, *Tubular reactor for liquid-phase propylene polymerization* (University of Twente [Host], 2006).

[6] A. G. Oliveira, P. M. Candreva, P. A. Melo, and J. C. Pinto, *Steady-state behavior of slurry and bulk propylene polymerization,* Polymer Reaction Engineering **11**, 155 (2003).

[7] S. Serranti, V. Luciani, G. Bonifazi, B. Hu, and P. C. Rem, *An innovative recycling process to obtain pure polyethylene and polypropylene from household waste,* Waste management **35**, 12 (2015).

[8] D. S. Achilias, P. Megalokonomos, and G. P. Karayannidis, *Current trends in chemical recycling of polyolefins,* (2006).

[9] https://www.eia.doe.gov.

[10] M. Al-Maadeed, Y. M. Shabana, and P. N. Khanam, *Processing, characterization and modeling of recycled polypropylene/glass fibre/wood flour composites,* Materials & Design **58**, 374 (2014).

[11] L. G. Barbosa, M. Piaia, and G. H. Ceni, *Analysis of impact and tensile properties of recycled polypropylene,* (2017).

[12] B. L. Fernandes and A. J. Domingues, *Caracterizao mecnica de polipropileno reciclado para a indústria automotiva,* Polímeros **17**, 85 (2007).

[13] M. M. Raj, H. V. Patel, L. M. Raj, and N. K. Patel, *Studies on mechanical properties of recycled polypropylene blended with virgin polypropylene,* International Journal of Science Innovations Today **2**, 194 (2013).

[14] . A. Jansson, K. Möller, and T. Gevert], *Degradation of post-consumer polypropylene materials exposed to simulated recycling—mechanical properties,* Polymer Degradation and Stability (2003).

[15] B. Lotz, J. Wittmann, and A. Lovinger, *Structure and morphology of poly (propylenes): a molecular analysis,* Polymer **37**, 4979 (1996).

[16] S. V. Meille and S. Brückner, *Non-parallel chains in crystalline γ-isotactic polypropylene,* Nature **340**, 455 (1989).

[17] K. Balani, V. Verma, A. Agarwal, and R. Narayan, *Biosurfaces: a materials science and engineering perspective* (John Wiley & Sons, 2015).

[18] R. J. Samuels and R. Y. Yee, *Characterization of the structure and organization of β-form crystals in type iii and type iv isotactic polypropylene spherulites,* Journal of Polymer Science Part A-2: Polymer Physics **10**, 385 (1972).

[19] F. Padden Jr and H. Keith, *Crystallization in thin films of isotactic polypropylene,* Journal of Applied Physics **37**, 4013 (1966).

[20] A. Khalina, E. Zainuddin, and I. Aji, *Rheological behaviour of polypropylene/kenaf fibre composite: effect of fibre size,* in *Key Engineering Materials*, Vol. 471 (Trans Tech Publ, 2011) pp. 513–517.

[21] Z. Zhou, Y. Zhang, Y. Zhang, and N. Yin, *Rheological behavior of polypropylene/octavinyl polyhedral oligomeric silsesquioxane composites,* Journal of Polymer Science Part B: Polymer Physics **46**, 526 (2008).

[22] H.-Y. Mi, X. Jing, and L.-S. Turng, *Fabrication of porous synthetic polymer scaffolds for tissue engineering,* Journal of Cellular Plastics **51**, 165 (2015).

[23] L. W. McKeen, *Effect of Temperature and Other Factors on Plastics and Elastomers, The. PDL Handbook Series* (Elsevier Science & Technology, 2007).

[24] T. Bremner, A. Rudin, and D. Cook, *Melt flow index values and molecular weight distributions of commercial thermoplastics,* Journal of Applied Polymer Science **41**, 1617 (1990).

[25] T. Ogawa, *Effects of molecular weight on mechanical properties of polypropylene,* Journal of applied polymer science **44**, 1869 (1992).

[26] H. Jmal, N. Bahlouli, C. Wagner-Kocher, D. Leray, F. Ruch, J.-N. Munsch, and M. Nardin, *Influence of the grade on the variability of the mechanical properties of polypropylene waste,* Waste Management **75**, 160 (2018).

[27] M. Ha, B. Kim, and E. Kim, *Effects of dispersed phase composition on thermoplastic polyolefins,* Journal of applied polymer science **93**, 179 (2004).

[28] J. Aurrekoetxea, M. Sarrionandia, I. Urrutibeascoa, and M. L. Maspoch, *Effects of recycling on the microstructure and the mechanical properties of isotactic polypropylene,* Journal of materials science **36**, 2607 (2001).

[29] J. Randall and E. Hsieh, *13c nmr in polymer quantitative analyses,* (ACS Publications, 1984).

[30] C. De Rosa and F. Auriemma, *Structural- mechanical phase diagram of isotactic polypropylene,* Journal of the American Chemical Society **128**, 11024 (2006).

[31] F. Auriemma, C. De Rosa, T. Boscato, and P. Corradini, *The oriented γ form of isotactic polypropylene,* Macromolecules **34**, 4815 (2001).

[32] C. De Rosa, F. Auriemma, T. Circelli, and R. M. Waymouth, *Crystallization of the α and γ forms of isotactic polypropylene as a tool to test the degree of segregation of defects in the polymer chains,* Macromolecules **35**, 3622 (2002).

[33] F. Auriemma and C. De Rosa, *Crystallization of metallocene-made isotactic polypropylene: Disordered modifications intermediate between the α and γ forms,* Macromolecules **35**, 9057 (2002).

[34] L. Resconi, L. Cavallo, A. Fait, and F. Piemontesi, *Selectivity in propene polymerization with metallocene catalysts,* Chemical Reviews **100**, 1253 (2000).

[35] H. Hinsken, S. Moss, J.-R. Pauquet, and H. Zweifel, *Degradation of polyolefins during melt processing,* Polymer degradation and stability **34**, 279 (1991).

[36] S. Luzuriaga, J. Kovářová, and I. Fortelnỳ, *Degradation of pre-aged polymers exposed to simulated recycling: properties and thermal stability,* Polymer Degradation and Stability **91**, 1226 (2006).

[37] https://www.custompartnet.com/wu/InjectionMolding.

[38] https://www.oberk.com/packaging-crash-course/packaging-resource-guide/plastic-closure-manufacturing-process.

[39] https://www.efunda.com/processes/plasticmolding/moldingcompression.cfm/.

[40] R. Haward and G. . Thackray, *The use of a mathematical model to describe isothermal stress-strain curves in glassy thermoplastics,* Proceedings of the Royal Society of London. Series A. Mathematical and Physical Sciences **302**, 453 (1968).

[41] S. G. Bardenhagen, M. G. Stout, and G. T. Gray, *Three-dimensional, finite deformation, viscoplastic constitutive models for polymeric materials,* Mechanics of Materials **25**, 235 (1997).

[42] J. Johnsen, A. H. Clausen, F. Grytten, A. Benallal, and O. S. Hopperstad, *A thermo-elasto-viscoplastic constitutive model for polymers,* Journal of the Mechanics and Physics of Solids **124**, 681 (2019).

[43] R. Thackray, *The use of a mathematical model to describe isothermal stress-strain curves in glassy thermoplastics,* Proceedings of the Royal Society of London **302**, 453 (1968).

[44] A. G. Holzapfel, *Nonlinear solid mechanics ii,* John Wiley Sons Inc (2000).

[45] T. Ree and H. Eyring, *Theory of non-newtonian flow. ii. solution system of high polymers,* Journal of Applied Physics **26**, 800 (1955).

[46] Ellen, M., Arruda, , , Mary, C., and Boyce, *A three-dimensional constitutive model for the large stretch behavior of rubber elastic materials,* Journal of the Mechanics Physics of Solids (1993).

[47] C. Miehe, *Entropic thermoelasticity at finite strains. aspects of the formulation and numerical implementation,* Computer Methods in Applied Mechanics and Engineering **120**, 243 (1995).

[48] L. Anand, *A constitutive model for compressible elastomeric solids,* Computational Mechanics **18**, 339 (1996).

[49] A. O. Cifuentes and A. Kalbag, *A performance study of tetrahedral and hexahedral elements in 3-d finite element structural analysis,* Finite Elements in Analysis and Design (ISSN 0168-874X), vol. 12, no. 3-4, p. 313-318. (1992).

[50] https://abaqus-docs.mit.edu/2017/English/SIMACAEANLRefMap/simaanl-c-expdynamic.htm.

[51] A. Wal, J. J. Mulder, H. A. Thijs, and R. J. Gaymans, *Fracture of polypropylene,* Polymer **39**, 5477 (1998).